23040 symmetries of hyperbolic tetrahedra

Peter Doyle Gregory Leibon

February 1, 2008

Abstract

We give a rigorous geometric proof of the Murakami-Yano formula for the volume of a hyperbolic tetrahedron. In doing so, we are led to consider *generalized hyperbolic tetrahedra*, which are allowed to be non-convex, and have vertices 'beyond infinity'; and we uncover a group, which we call $22.5\mathrm{K}$, of $23040 = 30 \cdot 12 \cdot 2^6$ scissors-class-preserving symmetries of the space of (suitably decorated) generalized hyperbolic tetrahedra. The group $22.5\mathrm{K}$ contains the Regge symmetries as a subgroup of order $144 = 12 \cdot 12$. From a generic tetrahedron, $22.5\mathrm{K}$ produces 30 distinct generalized tetrahedra in the same scissors class, including the 12 honest-to-goodness tetrahedra produced by the Regge subgroup. The action of $22.5\mathrm{K}$ leads us to the Murakami-Yano formula, and to 9 others, which are similar but less symmetrical. From here, we can derive yet other volume formulas with pleasant algebraic and analytical properties. The key to understanding all this is a natural relationship between a hyperbolic tetrahedron and a pair of ideal hyperbolic octahedra.

1 Introduction

The computation and understanding of hyperbolic volume is an old and difficult problem. Of fundamental interest and importance has been the exploration of the volume of the hyperbolic tetrahedron. In particular, historically there has been great interest in finding formulas for the tetrahedron's volume which have optimal algebraic simplicity, together with a concrete geometric interpretation (see Milnor [5], Kellerhals [4], and the references therein).

For the special case of an ideal hyperbolic tetrahedron, Milnor [5] presents and derives, in a straight-forward geometric way, what we presume is the optimally elegant volume formula. (See section 1.1.2 below.)

For a general hyperbolic tetrahedron, Murakami and Yano [8] recently found what we consider the most elegant known volume formula. (See section 1.1.3

below.) This formula arose from attempts to resolve Kashaev's conjecture that the colored Jones polynomials of a hyperbolic knot determines the hyperbolic volume of the knot's complement. It was discovered utilizing properties of the quantum $6j$-symbols, and justified by means of a known formula for hyperbolic volume due to Cho and Kim (see [1]). Murakami-Yano's derivation of their formula was formal and was lacking a concrete geometric interpretation. One goal of this paper is to provide a rigorous geometric interpretation, and explore several new views of tetrahedral volume.

1.1 Volume Formulas

Most of the formulas in this paper will be described as the volume of a specified scissors congruence class, hence we will first recall this concept.

1.1.1 Scissors Congruence

In this section we review the concept of scissors congruence and fix the notation that we will use in order to describe a scissors class. To articulate the notion of scissors congruence needed in this paper, we first form the free Abelian group, $\mathcal{F}$, generated by the symbols P, one for each (unoriented) geodesic polyhedron $P \subset H^3$. Let

$$\mathcal{R} = \langle P + Q - R, \sigma(S) - S \rangle ,$$

where the geodesic polyhedra P and Q have an intersection with empty interior and a union with interior equal to the interior of the geodesic polyhedron R, and where σ is an orientation preserving isometry being applied to a geodesic polyhedron S. The *scissors congruence group*, $\mathcal{P}(H^3)$, is isomorphic to the quotient group $\mathcal{F}/\mathcal{R}$. Notice that the volume, extended to $\mathcal{F}$ by linearity, provides a well defined homomorphism

$$\mathcal{V} : \mathcal{P}(H^3) \to \mathbf{R}.$$

We call any pair of elements in $\mathcal{F}$ that agree in $\mathcal{P}(H^3)$ *scissors congruent*. Given a geodesic polyhedron P we will let $[P]^s$ denote its scissors class.

There are a pair of observations about scissors classes that will be useful in what follows. First, Dupont and Sah proved that we may divide by 2 in $\mathcal{P}(H^3)$ (see [2]). In other words,

$$\begin{array}{rl} \text{if} & 2[P] = 2[Q], \\ \text{then} & [P] = [Q]. \end{array} \tag{1}$$

The second concerns a geodesic polyhedron's mirror image. Given a geodesic polyhedron P let P^* denote its mirror image. We have that

$$[P]^s = [P^*]^s, \tag{2}$$

as was noted in a letter to Gauss from Gerling in 1844 (see Neumann [10]).

Notice that the generators of $\mathcal{F}$ have no orientation associated to them, hence the scissors class $[P]^s$ will ignore any orientation data associated to P. If we are given an oriented convex polyhedron P, then we will let $[P] = [P]^s$ if P is positively oriented and let $[P] = -[P]^s$ if P is negatively oriented. We extend this to lists of oriented convex polyhedra by letting by letting

$$[(P_1, \ldots, P_M)] = \sum_{i=1}^{M} [P_i].$$

1.1.2 The Ideal Tetrahedron

Our scissors classes will always be closely related to a collection of oriented ideal tetrahedra. In this section, we fix some notation related to describing the ideal tetrahedron and review several useful facts concerning the ideal tetrahedron.

Recall that an unoriented ideal tetrahedron is the convex hull of 4 ideal points in hyperbolic space H^3. In order to describe this tetrahedron's orientation, and put coordinates on the collection of all such tetrahedra, it is useful to label this unoriented ideal tetrahedron. To do so we may label the ideal tetrahedron's four faces as in figure 1. For an ideal tetrahedron, this turns out to be more labeling than necessary, namely we can form coordinates which will only depend on the orientation class of the $\langle\{1\},\{2\},\{3\},\{4\}\rangle$ labeling and the specification of an edge. We can do this via the ideal tetrahedron's *complex coordinate*, $z(\{ij\})$, associated to the specified $\{ij\}$ edge. To compute $z(\{ij\})$, note that the sphere at infinity is naturally the Riemann Sphere, and $z(\{ij\})$ can be computed as the cross ratio of our ideal tetrahedron's four ideal points as

$$z(\{ij\}) \quad = \quad (\{ijl\},\{ijk\};\{jkl\},\{ikl\}),$$

where $\langle\{i\},\{j\},\{k\},\{l\}\rangle$ is in $\langle\{1\},\{2\},\{3\},\{4\}\rangle$ positive orientation class and where we have labeled our four ideal points as in figure 1.

If $z(\{14\})$ is denoted as z, then the edge choice dependency is determined as follows

$$z(\{14\}) = z(\{23\}) = z, \tag{3}$$

$$z(\{12\}) = z(\{13\}) = (z-1)/z, \tag{4}$$

$$z(\{13\}) = z(\{24\}) = 1/(1-z). \tag{5}$$

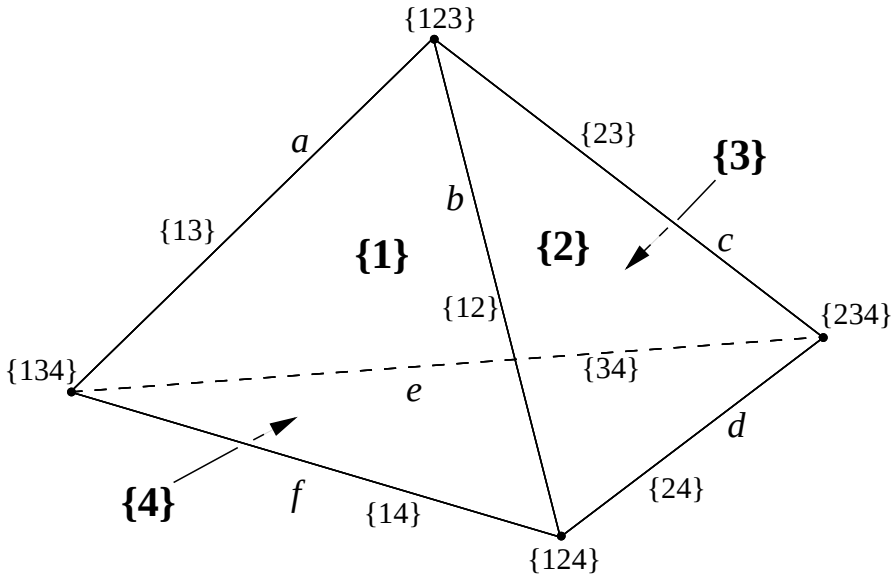

Figure 1: We will utilize an abstract simplex in order to *label* the hyperbolic tetrahedra which arise in this paper. To do so, view the simplex as the subsets of $\{1,2,3,4\}$, and identify each subset in the form $\{i\}$ with a tetrahedral face. The edge determined by $\{i\}$ and $\{j\}$ will be identified with the subset $\{i,j\}$, or $\{ij\}$ for short. Similarly, the vertex determined by $\{i\}$,$\{j\}$, and $\{k\}$ will be identified with the with the subset $\{i,j,k\}$, or $\{ijk\}$ for short. We will orient our simplex and let $\langle\{1\},\{2\},\{3\},\{4\}\rangle$ denote the positive orientation class. As such, for any finite or ideal hyperbolic tetrahedron, to each $\{ij\}$ will may assign a dihedral angle, $\theta(\{ij\})$. We will call $e^{i\theta(\{ij\})}$ the *circulant* associated to $\{ij\}$ and we will call $e^{2i\theta(\{ij\})}$ the *clinant* associated to $\{ij\}$. We have labeled the *tetrahedral clinants*, and will denote them as (a,b,c,d,e,f), while the circulants will be denoted as $\mathbf{c} = (\mathrm{A},\ \mathrm{B},\mathrm{C},\mathrm{D},\mathrm{E},\mathrm{F})$ and the dihedral angles will be denoted as $\mathbf{a} = (\mathcal{A},\mathcal{B},\mathcal{C},\mathcal{D},\mathcal{E},\mathcal{F})$.

Such an ideal tetrahedron has a natural orientation which can be easily determined by looking at the sign of any $\Im(z(\{ij\})$; if $\Im(z(\{ij\})$ is positive then the ideal tetrahedron is positively oriented and if $\Im(z(\{ij\})$ is negative then the ideal tetrahedron is negatively oriented. If $\Im(z(\{ij\})$ is 0, then the tetrahedron is degenerate, see the note at the end of this section. These concepts are independent of the choice of $\{ij\}$. Any permutation of the $\{i\}$ labels associated to $\langle\{1\},\{2\},\{3\},\{4\}\rangle$'s negative orientation class, negates the orientation. Using our above z, after reversing the orientation class, we have that

$$z(\{14\}) = z(\{23\}) = 1/z, \tag{6}$$

$$z(\{12\}) = z(\{34\}) = (1-z), \tag{7}$$

$$z(\{13\}) = z(\{24\}) = (z-1)/z. \tag{8}$$

In order to compute the orientation-sensitive volume of the ideal tetrahedron, we introduce the dilogarithm function

$$\mathcal{L}_2(z) = -\int_0^z \frac{\log(1-s)}{s} ds,$$

which can be viewed as an analytic function with a branch cut along $[1,\infty]$; and the Bloch-Wigner dilogarithm function

$$\mathcal{B}(z) = \Im(\mathcal{L}_2(z)) + \arg(1-z)\log|z|.$$

The volume is given by

$$\mathcal{V}([z(\{ij\}]) \quad = \quad \mathcal{B}(z(\{ij\}), \tag{9}$$

as derived by S. Bloch and D. Wigner and presented by Milnor in [6].

We can express the complex coordinate of an ideal tetrahedron in terms of the ideal tetrahedron's clinants via the the following observation

$$z(\{ij\}) \quad = \quad \frac{1-e^{-2i\theta(\{ik\})}}{1-e^{2i\theta(\{il\})}}, \tag{10}$$

where $\langle\{i\},\{j\},\{k\},\{l\}\rangle$ is in $\langle\{1\},\{2\},\{3\},\{4\}\rangle$ positive orientation class. Using the notation from figure 1, a labeled oriented ideal tetrahedron is equivalent to a list of clinants (a,b,c,a,b,c) where $abc=1$, which will be denoted as $(a,b,c)_{it}$. Once again, this coordinate is determined by the orientation class of the facial labeling and the specified edge, which corresponds to $(a,b,c)_{it}$'s first coordinate. The

edge changes in equations (3)-(5) correspond to even permutations of the $(a,b,c)_{it}$ coordinates, while orientation class changes in equations (6)-(8) correspond to the odd permutations together with the conjugation of all the clinants. Given any orientation reversing hyperbolic isometry I,

$$I((a,b,c)_{it}) \quad = \quad (\bar{a},\bar{b},\bar{c})_{it} \tag{11}$$

and, hence, by equation (2)

$$[(\bar{a},\bar{b},\bar{c})_{it}] \quad = \quad -[(a,b,c)_{it}]. \tag{12}$$

Notice this implies that all permutations of the $(a,b,c)_{it}$ coordinates preserve $[(a,b,c)_{it}]$, though the odd permutations require equation (2) and correspond to the original tetrahedron's positively oriented mirror image. In terms of the z coordinates, $I(z(\{14\})) = \bar{z}$, while $1/\bar{z}$ corresponds to the tetrahedron's positively oriented mirror image.

A particularly interesting special case of the ideal tetrahedron is the *isosceles* ideal tetrahedron

$$(d^2,-1/d,-1/d)_{it}.$$

Equivalently, an ideal tetrahedron is isosceles if its complex coordinate is unit sized. In fact, for $(d^2,-1/d,-1/d)_{it}$ we have $z(\{14\}) = d$, hence, from equation (9),

$$\mathcal{V}([(d^2,-1/d,-1/d)_{it}]) = \Im(\mathcal{L}_2(d)).$$

It is geometrically straight-forward (see Milnor [5]) to prove that

$$2[(a,b,c)_{it}] = [(a^2,-1/a,-1/a)_{it},(b^2,-1/b,-1/b)_{it},(c^2,-1/c,-1/c)_{it}], \tag{13}$$

hence

$$\mathcal{V}(2[(a,b,c)_{it}]) \quad = \quad \Im(\mathcal{L}_2(a)+\mathcal{L}_2(b)+\mathcal{L}_2(c)). \tag{14}$$

Comment: Letting $\mathcal{D} = \frac{arg(d)}{2}$, we have that

$$\frac{1}{2}\Im(\mathcal{L}_2(d)) = \Lambda(\mathcal{D}),$$

where $\Lambda(x)$ is the Lobachevsky function. Hence, as observed by Milnor (see [5]), we may express equation (14) as

$$\mathcal{V}([(a,b,c)_{it}]) \quad = \quad \Lambda(\mathcal{A})+\Lambda(\mathcal{B})+\Lambda(\mathcal{C}).$$

Note: If we compactify the space of ideal tetrahedra there are three types of degenerate tetrahedra, the ***flattened*** ideal tetrahedra, where $z(\{ij\})$ is real and not

in $\{0, 1, \infty\}$, and the *stretched* ideal tetrahedra, corresponding to a permutation of $(1, d, 1/d)_{it}$ where $d \neq 1$, and the stretched and flattened tetrahedra where $d = 1$ and $z(\{ij\}) \in \{0, 1, \infty\}$. The space of all oriented ideal tetrahedra with a specified edge can be described by the blowing up of $S^1 \times S^1$ with center the point $(1, 1)$. In other words the real analytic variety formed by taking $S^1 \times S^1$ and replacing $(1, 1)$ with the set of lines through $(1, 1)$. To accomplish this we view $(a, b) \in S^1 \times S^1$ as a pair of clinants. If $a \neq 1$ and $b \neq 1$, then $(a, b, c)_{it} = (a, b, 1/(ab))_{it}$. When $(a, b) = (1, 1)$ the slopes of the lines through $(1, 1)$ correspond to the real valued complex coordinates via equation (10).

1.1.3 The Murakami-Yano formula

Here we present the Murakami-Yano formula using the notation from sections 1.1.1 and 1.1.2. We will use the tetrahedral circulants as described in figure 1, and, throughout this subsection, and the next, we let $\mathbf{c} = (\text{A}, \text{B}, \text{C}, \text{D}, \text{E}, \text{F})$ be the tetrahedral circulants of a finite hyperbolic tetrahedron, which we shall denote as $(\mathbf{c})_{tet}$. Let $p = \text{ABC}$, $q = \text{DEF}$,

$$\alpha(\mathbf{c}) = 2\left(\text{AD} + \text{BE} + \text{CF} + pq + p\left(\text{D}/\text{A} + \text{E}/\text{B} + \text{F}/\text{C} + q/p\right)\right),$$

$$\beta(\mathbf{c}) = (\text{D}/\text{A}+\text{E}/\text{B}+\text{F}/\text{C}+\text{A}/\text{D}+\text{B}/\text{E}+\text{C}/\text{F})-(\text{AD}+\text{BE}+\text{CF}+1/(\text{AD})+1/(\text{BE})+1/(\text{CF})),$$

and

$$\delta(\mathbf{c}) = |\alpha|^2 - \beta^2.$$

In section 2.2, we shall find that δ is always positive, hence, using the positive square root, we may define the unit sized complex number

$$\rho(\mathbf{c}) \quad = \quad \frac{-\beta - i\sqrt{\delta}}{\alpha}. \tag{15}$$

Using ρ, we define the following list of isosceles ideal tetrahedra

$$(\mathbf{c})_{\text{MY}} \quad = \quad \left(\overline{\rho}, -\rho_{\text{CDE}}, \overline{\rho_{\text{BCEF}}}, -\rho_{\text{AEF}}, \overline{\rho_{\text{ACDF}}}, -\rho_{\text{ABC}}, \overline{\rho_{\text{ABDE}}}, -\rho_{\text{BDF}}\right).$$

Murakami and Yano derive the following formula (see [8]):

$$\mathcal{V}\left(4\left[(\mathbf{c})_{tet}\right]\right) \quad = \quad \mathcal{V}\left(\left[(\,\mathbf{c}\,)_{\text{MY}}\right] + \left[(\bar{\mathbf{c}})_{\text{MY}}\right]\right). \tag{16}$$

We give an alternate proof of the Murakami-Yano formula by proving the following theorem.

Theorem 1 *Generically*

$$4\left[(\mathbf{c})_{tet}\right] = \left[(\,\mathbf{c}\,)_{MY}\right] + \left[(\bar{\mathbf{c}})_{MY}\right].$$

Sketch of Proof: Here we describe how to geometrically realize this scissors congruence. That we arrive at the correct angles, and that all the steps in this construction are well defined, is verified in section 2. Throughout this sketch, terminology is used which hopefully will be clear to the reader from the indicated figures.

The first step in this construction is summed up in figure 2 and its caption, which is a geometric summary of part 2 of theorem 4 from section 2.1. In figure 2, we see that the $2[(\mathbf{c})_{tet}]$ in the first row is equivalent to the scissors class of the pair of octahedra in the bottom row. We will call these octahedral a pair of *octahedral buddies*, a concept we develop carefully in section 2.2. It is also convenient to name the regions in the second row of figure 2. We will call these regions *supertetrahedra*, as introduced in figure 6. Notice in figure 2, that we utilized the cutting down procedure witnessed in figure 8 to *cut down* our supertetrahedra in row 2 to the octahedral buddies in row 3. In describing this cutting down procedure, we utilize the convex version of the supertetrahedron. This ability to use the convex case as a template for our constructions will prove very useful, and, in section 2.1, we develop the notion a *C-region* to carefully justify this technique. In order to appreciate the utility of not needing to explicitly work outside the convex case, we invite the reader to attempt to explicitly perform the cut downs in going from the supertetrahedra in the second row of figure 2 to the octahedra in the third row.

Once we have our octahedral buddies, we can perform the *puff-and-cut* developed in figure 11 with respect to any choice of vertex and face at this specified vertex. Performing this operation simultaneously to our octahedral buddies in row 3 of figure 2, utilizes a pair of oppositely oriented ideal tetrahedra pairs. Hence, this puff-and-cut does not affect the scissors class of our octahedral buddies. In fact, a puff-and-cut is independent of whether we use our specified face or the face opposite to our specified face at our specified vertex. Hence, using the shading in figure 10, we can index our puff-and-cuts as P^s_v or P^u_v, depending on whether we use the shaded or unshaded pair of faces at v. If we apply

$$g_o \;=\; P^s_{\{14\}}P^s_{\{13\}}P^u_{\{34\}}P^s_{\{14\}}P^s_{\{23\}}P^s_{\{34\}}P^s_{\{12\}} \tag{17}$$

to our octahedral buddies in the final row of figure 2, then, as a scissors class, we have produced 8 ideal tetrahedra. At this point, we double these 8 ideal tetrahedra, and, use equation (13) to express these doubled ideal tetrahedra as 24 isosceles ideal tetrahedra. We find that 8 of these 24 isosceles ideal tetrahedra occur as pairs consisting of an isosceles ideal tetrahedron together with an oppositely oriented copy of this isosceles ideal tetrahedron. Hence $4[(\mathbf{c})_{tet}]$ is equal to the remaining 16 isosceles ideal tetrahedra. In section 2, we compute the angles arising in these 16 isosceles ideal tetrahedra and find these tetrahedra are precisely $[(\,\mathbf{c}\,)_{\mathrm{MY}}] + [(\,\bar{\mathbf{c}}\,)_{\mathrm{MY}}]$, our needed scissors class.

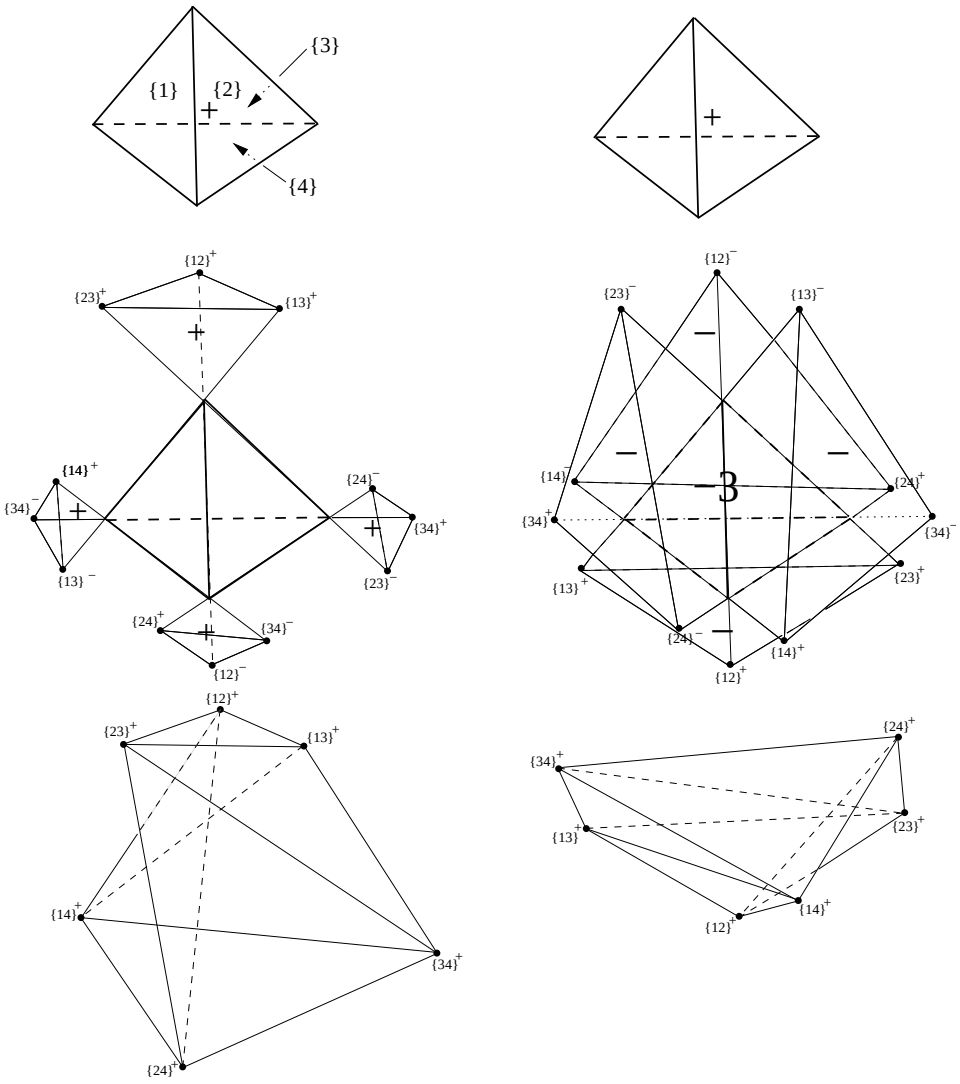

Figure 2: We start in the top row with two copies of our finite tetrahedron. We then adjoin to the left hand copy the four indicated tetrahedra where the bold faced vertices are ideal. To the right hand copy we remove the four indicated tetrahedra. The four adjoined and the four removed tetrahedra cancel out as a scissors classes by equation (2). The resulting regions in the second row can be cut down to the octahedra with the $\{ij\}^+$ vertices by removing the 6 ideal tetrahedra corresponding to the $\{ij\}^-$ vertices. The combinatorics of our removal process is seen in figure 8, where we find that the ideal tetrahedra being removed cancel in pairs. Hence, we have realized $2[(\mathbf{c})_{tet}]$ as the scissors class of the pair of octahedra in the bottom row.

q.e.d

Comment 1: The term 'generically' in the statement of theorem 1 refers to the fact that theorem 1 is only proved for the finite hyperbolic tetrahedra in an open dense set of the space of finite hyperbolic tetrahedra. In section 2.4 we describe the exact restrictions on our tetrahedra. Despite this caveat, by continuity of volume, theorem 1 implies that equation (16) will hold for all tetrahedra.

Comment 2: Murakami and Yano expressed the needed $\rho(\mathbf{c})$ and $\rho(\bar{\mathbf{c}})$ using the roots of the quadratic polynomial

$$h(\mathbf{c}, z) \quad = \quad \alpha z^2 + 2\beta z + \bar{\alpha}$$

or, more precisely, the roots of $\frac{\text{ABCDEF}}{2} h(\mathbf{c}, z)$, which can be written as

$$\begin{aligned} \frac{\text{ABCDEF}}{2} h(\mathbf{c}, z) \quad = \quad & -1/z \left((1-z)(1-\text{ABDE}z)(1-\text{ACDF}z)(1-\text{BCEF}z) \right. \\ & \left. -(1+\text{ABC}z)(1+\text{AEF}z)(1+\text{BDF}z)(1+\text{CDE}z) \right). \end{aligned}$$

Notice that the two roots of $h(\mathbf{c}, z)$ are $\rho(\mathbf{c})$ and $\overline{\rho\left(\bar{\mathbf{c}}\right)}$.

1.1.4 Alternate Views of Hyperbolic Volume

One of the achievements of the Murakami-Yano formula was that it reduced the algebraic difficulty of volume computation to a quadratic equation. Namely, the Murakami-Yano formula reduces the algebraic difficulty of computing volume to choosing the appropriate square root of $\delta(\mathbf{c})$ in equation (15). We now describe how to analytically factor this $\sqrt{\delta}$ out of the volume equation altogether, further revealing the algebraic and analytic simplicity of hyperbolic volume. To do so, let γ_i be the i^{th} component of the following vector

$$\vec{\gamma} = [1, -\text{CDE}, \text{BCEF}, -\text{AEF}, \text{ACDF}, -\text{ABC}, \text{ABDE}, -\text{BDF}].$$

and

$$c_i = \frac{-i\gamma_i}{\alpha + \gamma_i \beta}.$$

We find there is an analytic function $\mathcal{F}$ such that

$$\mathcal{V}([(\mathbf{c})_{tet}]) \quad = \quad \Im \left(\frac{\sqrt{\delta}}{2} \sum_{i=1}^{8} (-1)^i c_i \mathcal{F}\left(\delta c_i^2\right) \right). \tag{18}$$

To describe $\mathcal{F}$, let

$$\mathcal{H}(w) \quad = \quad \mathcal{L}_2\left(\frac{2w}{1+w}\right) + \frac{1}{4}\left(\log\left(\frac{1-w}{1+w}\right)\right)^2$$

with branch cuts $[-\infty, 1] \bigcup [1, \infty]$ and $H(0) = 0$. In section 3.1, we will see that

$$\mathcal{V}(2[(\mathbf{c})_{tet}]) \quad = \quad \Im\left(\sum_{i=1}^{8}(-1)^i \mathcal{H}(c_i\sqrt{\delta})\right). \tag{19}$$

In section 3.2, we will check that $H(w)$ is odd, which immediately implies equation (18).

In section, 3.3 several other views of the formula for hyperbolic volume are explored.

1.2 Scissors Congruences of the Tetrahedron

At the heart of the proof of theorem 1 is the construction of the transformation g_o from equation (17). The puff-and-cuts used to build g_o generate a group of scissors congruences, which we will discuss in this section. To make good sense out this group, we first develop the notion of a *generalized hyperbolic tetrahedron.*

1.2.1 The Generalized Hyperbolic Tetrahedron

Generalized hyperbolic tetrahedra are oriented, labeled subsets of hyperbolic space, that include, as a special case, the finite hyperbolic tetrahedra. The generalized hyperbolic tetrahedra should be viewed as the natural analytic continuation of the space of finite hyperbolic tetrahedra. To make these tetrahedra less mysterious we have the following result.

Theorem 2 *Up to orientation preserving isometry, every collection of four, distinct, labeled, pairwise intersecting planes in H^3 corresponds to a unique generalized hyperbolic tetrahedron.*

Sketch of Proof: This theorem is proved in section 2.1, where the generalized hyperbolic tetrahedron is carefully developed. Throughout this sketch, various terminology is used which hopefully will be clear to the reader from the indicated figures.

Notice that the labeling scheme from figure 1 can be used to label any collection of four, distinct, labeled, pairwise intersecting planes in H^3. As such, we call each plane $\{i\}$ a *tetrahedral face*, each geodesic $\{ij\}$ when $i \neq j$ a *tetrahedral edge* and each $\{ijk\}$ a *tetrahedral vertex*, when $\{ijk\}$ is nonempty and i,j,and k are distinct. We will find that a bit more labeling is sometimes desirable, and we will say that such a labeled collection of planes is *decorated* if each geodesic $\{ij\}$ has been assigned an orientation. This is equivalent to labeling the two end points of $\{ij\}$ at infinity as $\{ij\}^+$ and $\{ij\}^-$.

Our first step of this proof will be to construct the general supertetrahedron, a concept introduced in the sketch of theorem 1's proof. To do so, take any four planes as described in the statement of the above theorem and decorate them. A supertetrahedron can be constructed by attaching to the $\{ij\}^{\pm}$ ideal vertices the ideal tetrahedra witnessed in figure 8. A couple of examples of the sorts of regions that can result from this procedure are seen in the second row of figure 6.

From our supertetrahedron we can construct our needed generalized hyperbolic tetrahedron. We can motivate this construction by attempting to reverse, for any supertetrahedron, the process of turning the finite tetrahedra in row 1 of figure 2 into the supertetrahedra in row 2. The four tetrahedra utilized in figure 2 to go from row 1 to 2 are special cases of *half prisms*, see the second row of figure 5. In general, at each 'vertex' of a supertetrahedron there is well defined prism, see figure 5. Starting with a supertetrahedron, we can remove the top halves of these four prisms and call the resulting region a *generalized hyperbolic tetrahedron*, see figure 9. As in figure 2, we see that the finite tetrahedron is a special case of this construction.

At this point in the proof, we have associated a generalized hyperbolic tetrahedron to every collection of collection of four, distinct, decorated, pairwise intersecting planes in H^3. To finish this proof, we need to demonstrate that the region determined by this construction is independent of our the edge orientations provided by our decoration. This fact is discussed in figure 3, and figure 3's caption completes our sketch.

q.e.d

Theorem 1 holds, generically, for all generalized hyperbolic tetrahedra. From this point on, we will refer to a labeled generalized hyperbolic tetrahedron as a *hyperbolic tetrahedron*, or simply a *tetrahedron*. When we want to emphasize that a hyperbolic tetrahedron is finite, ideal or decorated we will say so. We will find that every tetrahedron can be assigned angle data as described in figure 1. We will let *tetrahedral angle data* refer to all six-tuples of real numbers modulo 2π that correspond to a tetrahedron's associated dihedral angles, denoted as $\mathbf{a} = (\mathcal{A}, \mathcal{B}, \mathcal{C}, \mathcal{D}, \mathcal{E}, \mathcal{F})$. This association will not be unique. Generically, there are 2^8 different collections of tetrahedral angle data that correspond to the same tetrahedron.

Comment: Using the planes associated to our tetrahedron, we may decorate a tetrahedron by decorating its associated planes, as defined in the sketch of theorem 2's proof. The space of decorated tetrahedra form a 2^6 fold cover of the space of tetrahedra. Decorating a tetrahedron resolves most of the ambiguity in associating tetrahedral angle data to its edges. Namely, there are only 4 different collections of tetrahedral angle data that correspond to the same decorated tetrahedron. They are all related by the copy of the Klein 4 group generated by adding π to all but an

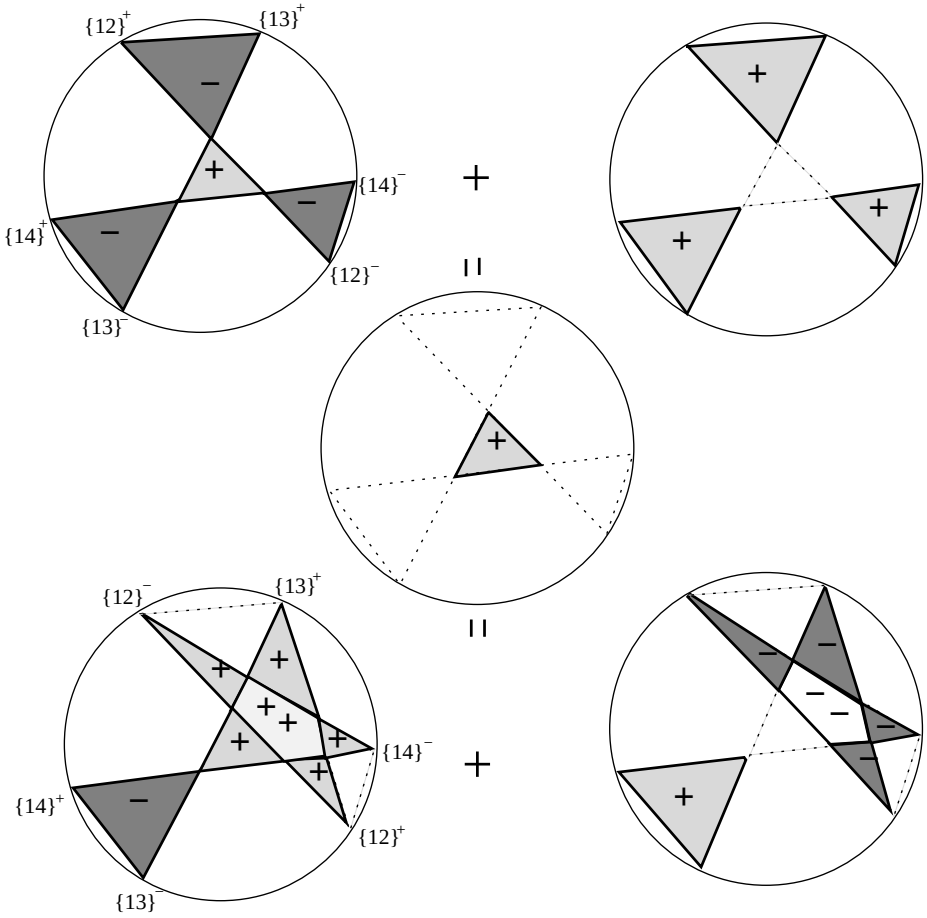

Figure 3: Here we describe why the construction of our generalized hyperbolic tetrahedron is independent of our $\pm$ sign choices. We will call the process of changing such a choice the process of *flipping an edge*. The flipping of an edge simultaneously modifies the supertetrahedron and the four prisms involved in the tetrahedron's construction. In the top row of his figure, we see what the supertetrahedron and three prisms on the left hand side of the second row in figure 2, look like in the $\{1\}$ plane before flipping the $\{12\}$ edge. In the bottom row of this figure, we see what the supertetrahedron and three prisms look like after flipping the $\{12\}$ edge. Notice that in both cases, our supertetrahedron and half prisms combine to together to form the tetrahedral face in the center of this figure. The fact that this is true in all the $\{i\}$ planes implies that flips preserve the needed tetrahedron (since two such regions that share the same boundary will share the same interior). These ideas will be carefully developed in section 2.1.

opposite pair of dihedral angles, or rather the negation of all but an opposite pair of circulants. We shall call this group K_4. Geometrically, K_4 plays no and in order to produce honest coordinates on the space of decorated tetrahedra will require modding out by K_4's action. Such coordinates are useful for a variety of technical reasons, and in section 2.3.2 we introduce them as the *balanced coordinates*.

1.2.2 Volume Preserving Transformations

We will say that g, a transformation acting on the space of tetrahedral angle data, as introduced in section 1.2.1, is a *volume-preserving transformation* if the volume of the tetrahedron with tetrahedral angle data $\mathbf{a}$ is the same as the volume of the tetrahedron with tetrahedral angle data $g \cdot \mathbf{a}$. One of the interesting corollaries of the Murakami-Yano formula is that the formula exposes the fact that the elements of the Regge group are hyperbolic volume-preserving transformations. The Regge group was discovered originally as an order-144 group that preserves the classical $6j$-symbol. In order to describe the Regge symmetries, let

$$\mathcal{S} = \frac{\mathcal{B} + \mathcal{C} + \mathcal{E} + \mathcal{F}}{2}.$$

The Regge Group, viewed as acting on tetrahedral angle data, consist of the group generated by the tetrahedral symmetries together with the transformation g_r satisfying

$$g_r \cdot \mathbf{a} = (\mathcal{A}, \mathcal{S} - \mathcal{B}, \mathcal{S} - \mathcal{C}, \mathcal{D}, \mathcal{S} - \mathcal{E}, \mathcal{S} - \mathcal{F}).$$

Regge and Pozano conjectured that from the $6j$-symbols one can reconstruct the volume of a Euclidean polyhedron, which would imply that the Regge symmetries are, in fact, Euclidean volume-preserving transformations. Roberts resolved the Regge-Pozano conjecture and also observed that each of these symmetries is realized by a scissors congruence (see [9]). In particular, this allowed Roberts to construct 12 distinct tetrahedra scissors congruent to a fixed Euclidean tetrahedron (generically). To accomplish this Roberts utilizes the Dehn sufficiency theorem in Euclidean space (that volume and the Dehn invariant determine a scissors class, see Dupont and Sah [3]). In hyperbolic space, Dehn sufficiency remains one of the fundamental unsolved conjectures concerning the nature of hyperbolic volume (once again, see Dupont and Sah [3]). If the Hyperbolic Dehn Sufficiency Conjecture is true, then, from the Murakami-Yano formula, the Regge symmetries would be realized by scissors congruences. However, without a resolution to the Dehn sufficiency conjecture, proving that these symmetries are realized by scissors congruences will require other tools. By an explicit construction, Mohanty has proved that the Regge symmetries are scissors congruences (see [7] and the comment at the end of this section). As a scholium to our methods, we find that the Regge

symmetries are just the beginning. In section 2.3, we construct the group described in the following result.

Theorem 3 *There is an order-*23040 *group of scissors-class-preserving transformations acting properly on the space of decorated tetrahedra. We will call this group* $22.5\mathrm{K}$.

Sketch of Proof: In section 2.3, these constructions, and the reasoning behind them, is developed carefully.

First, we describe how to generate $22.5\mathrm{K}$ and why $22.5\mathrm{K}$'s elements induce scissors congruences. In section 2.3.2, we give a careful algebraic description of $22.5\mathrm{K}$. In particular, we find that $22.5\mathrm{K}$ is isomorphic to D_6, where D_6 is a well known order-23040 reflection group.

Let $22.5\mathrm{K}$ be the group generated by the puff-and-cuts from figure 11. We will view this group as acting on the set of all octahedral buddies. Octahedral buddies will have conjugate dihedral clinants, and, hence, the ideal tetrahedra involved in performing the puff-and-cut will pairwise cancel out, just as they did with respect the octahedral buddies arising in sketch of theorem 1's proof. In order to see how to apply $g \in G$ to a decorated tetrahedron, first apply the construction in figure 2, to realize the double of our tetrahedron as a pair of octahedral buddies. Notice, going from the first row to the second row in figure 2, is well defined in general since our decoration allows us to canonically associate a supertetrahedron to our tetrahedron, as in the sketch of theorem 2's proof. To these octahedral buddies apply g. This results in new octahedral buddies. We then invert the construction in figure 2, which produces a new (decorated) doubled tetrahedron. By construction, this new doubled tetrahedron is scissors congruent to its underlying octahedral buddies. Hence, the original doubled tetrahedron is scissors congruent to the new doubled tetrahedron, and, by equation (1), the tetrahedra themselves are scissors congruent.

q.e.d

In terms of volume-preserving transformations, we have the following corollary.

Corollary 1 *There is an order-*92160 *group of hyperbolic volume-preserving transformations acting properly on the space of tetrahedral angle data. We will call this group* $90\mathrm{K}$.

Proof: We can lift $22.5\mathrm{K}$'s action to a proper action on the tetrahedral angle data corresponding to decorated tetrahedra. For example, the g_o from equation (17) acts via

$$g_o \cdot \mathbf{a} = (-\mathcal{A}, -\mathcal{S}, \mathcal{E} + \mathcal{F} - \mathcal{S}, -\mathcal{D}, \mathcal{B} + \mathcal{E} - \mathcal{S}, \mathcal{B} + \mathcal{F} - \mathcal{S}).$$

This action determines most of $90\mathrm{K}$. However, as in the comment at the end of section 1.2.1, the space of tetrahedral angle data corresponding to decorated tetrahedra forms a four fold cover of the space of decorated tetrahedra, hence we should throw in the deck group of this cover. This is precisely the group K_4 from the comment at the end of section 1.2.1. K_4 commutes with our lifting of $22.5\mathrm{K}$'s action. Hence all the elements of $90\mathrm{K} = 22.5\mathrm{K} \times K_4$ correspond to volume-preserving transformations.

q.e.d

From the sketch of theorem 3's proof, we see that $22.5\mathrm{K}$ acts on the space of decorated tetrahedra. However, $22.5\mathrm{K}$ does not act (as a group) on the space of tetrahedra. This is because the edge flips, from figure 3, generate a subgroup of $22.5\mathrm{K}$ which preserves any tetrahedron but is not normal in $22.5\mathrm{K}$. This group generated by the edge flips is isomorphic to $\left(\frac{\mathbf{Z}}{2\mathbf{Z}}\right)^6$, called the *shaded subgroup*, and plays a fundamental in the proof of the following corollary.

Corollary 2 *There are generically 30 (generalized) tetrahedra scissors congruent to a fixed tetrahedron no pair of which are congruent to each other via an orientation preserving isometry.*

Proof: $22.5\mathrm{K}$ contains many elements which preserve a tetrahedron up to orientation preserving isometry. For one $22.5\mathrm{K}$ contains the tetrahedral symmetries, see section 2.3.3. $22.5\mathrm{K}$ also contains the shaded subgroup, which, in terms of its action on the tetrahedral angle data, corresponds to the negation of the individual coordinates. Let P be the order-$768 = 12 \cdot 2^6$ subgroup group of $22.5\mathrm{K}$ generated by the edge flips and the orientation preserving tetrahedral symmetries. The elements of $22.5\mathrm{K}/P$ are our 30 candidate tetrahedra. To see that these tetrahedra are distinct from our original tetrahedron, we will need that the cosines of 2 times the dihedral angles of each representative are well defined. This is guaranteed by lemma 1 and the fact that cosine is an even function. To finish our proof, we look at representatives of each of these 30 cossets and note that none (but the identity) have these cosines of 2 times their dihedral angles related to the original tetrahedron by an orientation preserving tetrahedral symmetry. To verify this requires looking at a representative of each of the 30 cosets of $22.5\mathrm{K}/P$. In section 2.3.3, we write down these cosets.

q.e.d

Comment: As discussed in section 1.2.1, among generalized tetrahedra the tetrahedral angle data is not well defined. However, among finite tetrahedra this concept is perfectly well defined. The problem is that $22.5\mathrm{K}$ will take finite tetrahedra to non-finite tetrahedra, and force us to give up this notion. In fact, if we start with a finite tetrahedron, then only 12 of the 30 tetrahedra from corollary 2

are finite tetrahedra (see section 2.4). These twelve tetrahedra correspond precisely to the Regge scissors classes. Mohanty produces a construction of the Regge symmetries, a construction where the notion of dihedral angle remains well defined throughout the process (see [7]).

2 Constructions

In this section, we carefully describe the geometric constructions necessary to prove theorems 1, 2, and 3. In our first section, we develop the notion of a generalized hyperbolic tetrahedron, as discussed in section 1.2.1.

2.1 The Generalized Hyperbolic Tetrahedron

Here we will construct the generalized hyperbolic tetrahedron needed to prove theorem 1. To do so we utilize the concept of a C-region. A C-region gives us a way of building non-convex regions of $\mathbf{H}^3$ utilizing a convex ideal polyhedron, C, as a template. These C-regions are technically very convenient, and, by utilizing them, one can construct an open dense subset of all hyperbolic tetrahedra, see comment 2 at the end of this section. Some of the results in this section are most naturally proved by induction from the one dimensional case, hence we will also discuss these notions in $\mathbf{H}^1$ and $\mathbf{H}^2$. In fact, all the results in this section have analogs in $\mathbf{H}^n$.

C-Regions, the idea: Intuitively, the C-region is simple to describe. Realize C as a chain of ideal tetrahedra. Viewing this chain as an abstract chain, a C-region is another realization of this chain with ideal tetrahedra, such that, if a collection of C's vertices all lived on a face of C, then the vertices are still cohyperplanar in the C-region. Examples of C-regions are given in figures 5 and 6, and are always denoted via a pair $|C, R|$, where C is the convex template and R denotes a realization of the template. The geometric region determined by $|C, R|$ (denoted as $||C, R||$), the scissors class determined by $|C, R|$ (denoted as $[C, R]$) and $|C, R|$'s dihedral clinants of are all well defined and independent of the chain used to realize C. This intuitive picture, along with these facts, should be enough to understand the constructions in this chapter, but here is a formal definition.

C-Regions, the definition: We will use the Klein model of $\mathbf{H}^3$, and, hence, may view any chain of hyperbolic tetrahedra with all finite and/or ideal vertices as a chain of Euclidean tetrahedra in $\mathbf{E}^3$. Let S be an finite oriented 3-dimensional simplicial complex. We let a *realization* R of S be an assignment of a point $R(p) \in \mathbf{E}^3$ for every vertex $p \in S$. A pair (S, R) will be called a *Euclidean chain* provided R is injective. We may simplicially extend R and continuously map our abstract

complex into $\mathbf{E}^3$, and, assign an integer *label* to a full measure set of points in $\mathbf{E}^3$ corresponding to the local degree of this mapping. This labeled set will be called the *region* determined by (S, R). If $R(p)$ is in the closed unit ball, then (S, R) may also be used to represent a well defined *Hyperbolic chain*, and the region determined by (S, R) can be thought of as a labeled subset of $\mathbf{H}^3$, which will be denoted as $||S, R||$. Let $[S, R]$ be the scissor class of the list of tetrahedra determined by (S, R). If all the vertices are ideal, then we call (S, R) an *ideal chain*. Utilizing the ideal tetrahedra used to form an ideal chain, we find that an ideal chain has a well defined scissors class and well defined dihedral circulants.

If C is a convex ideal polyhedron we may triangulate C using its ideal vertices, and, hence, realize C as $||S_C, R_C||$ for some ideal chain (S_C, R_C). Given an (S_C, R), if any set of vertices that shared a top dimensional facet in C are still cohyperplanar under R, then we will say that R satisfies C's *facial constraints*. We will let a *C-Region*, $|C, R|$, be an labeled subset of H^3 which is $||S_C, R||$ for some S_C where R satisfies C's facial constraints and where all of C's top dimensional facets determine distinct hyperplanes.

Lemma 1 *If $|C, R| = ||S_C, R||$, then any other chain, $\hat{S}_C$, used to realize C we have that $|C, R| = ||\hat{S}_C, R||$. Furthermore, $|C, R|$'s scissors class, $[S_C, R]$, and dihedral clinants are well defined, in other words, independent of the choice of S_C.*

Proof: Our goal will be to take any two chains S_C and $\hat{S}_C$ and to show that $[S_C, R] = [\hat{S}_C, R]$, $||S_C, R]|| = ||\hat{S}_C, R||$ and that the dihedral clinant agrees.

To begin, notice $\hat{S}_C$ induces a triangulation of each of C's faces. To such a triangulation we'd like to implement a sequence *22-moves*, where a 22-move takes two triangles that meet in the diagonal of a quadrilateral and replaces them with the triangles forming the quadrilateral that share the quadrilateral's other diagonal. It is simple to verify that every triangulation of a convex polygon utilizing only the polygon's vertices as vertices of the triangulation is equivalent to every other such triangulation via a sequence of such 22-moves. In n dimensions we have the analogous 2n-move, for example the 23-move in figure 4 , which also has this property.

The next observation is that the 22-moves of $\hat{S}_C$'s boundary can be implemented by adding or removing tetrahedra to a face of C. Since R satisfies C's facial constraints these tetrahedra are degenerate and hence will not change $[\hat{S}_C, R]$, $||\hat{S}_C, R||$ or any dihedral clinant. This procedure may change a dihedral circulant by -1, and hence the circulants will not be well defined. Utilizing these degenerate tetrahedron, and the observation that all the facial triangulations of C differ by 22-moves, assures us that we may, without loss of generality, assume that the triangulation of $\hat{S}_C$'s boundary agrees with the triangulation of S_C's boundary.

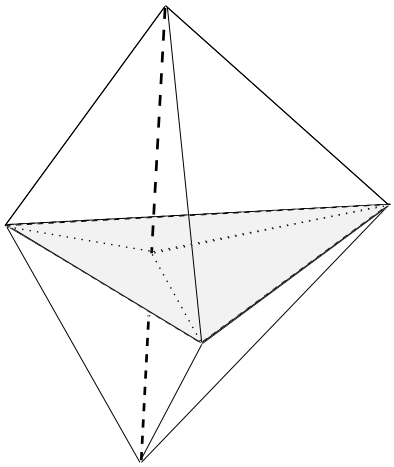

Figure 4: Here we see how to view a pair of tetrahedra glued along the shaded face as the triple of tetrahedra that share the bold edge, or conversely. Such a view point change is an example of a 23-move.

Since $\hat{S}_C$'s and S_C's boundary agree, we may glue together S_C to $-\hat{S}_C$ to form a sphere. R induces a mapping of S^3 into E^3 which must have degree zero, hence, $||S_C, R|| = ||\hat{S}_C, R||$ from which $[S_C, R] = [\hat{S}_C, R]$ immediately follows. Since the sphere is boudaryless the clinants around every edge must multiply to one, hence the dihedral clinants of $|S_C, R|$ and $|-\hat{S}_C, R|$ must be conjugate. The clinants of $|-\hat{S}_C, R|$ are conjugate of those of $|\hat{S}_C, R|$, hence, by equation (12), the clinants of $|\hat{S}_C, R|$ and $|S_C, R|$ must agree.

An independent proof can be accomplished by noticing that all triangulation of C are equivalent via a sequence of the *23-moves* in figure 4. In fact, the 23-move forms the primary relation in $\mathcal{P}(H^3)$, when $\mathcal{P}(H^3)$ is viewed as generated by ideal tetrahedra (see Dupont and Sah [2]).

q.e.d

Hyperplane Notation: In figures 5 and 6, we see our most important examples of C-regions, the prism and the supertetrahedron. We use hyperplanes to indicate our method of labeling the vertices. We use the labeling scheme described in the sketch of theorem 2's proof. We says $\{1, 2, 3, 4\}$ is a *non-degenerate* collection if each $\{ij\}$ with $i \neq j$ is one dimensional and if each $\{ijk\}$ fails to be an ideal point.

Flipping an Edge: With such a labeling we have the notion of *flipping an edge*, described in figure 3. In terms of our C-region notation, flipping the edge $\{ij\}$ correspond to changing the roles of $\{ij\}^+$ and $\{ij\}^-$. In other words, starting with $|C, R|$ we form $|C, F_{ij}R|$, where R and $F_{ij}R$ agree on all the vertices of S_C

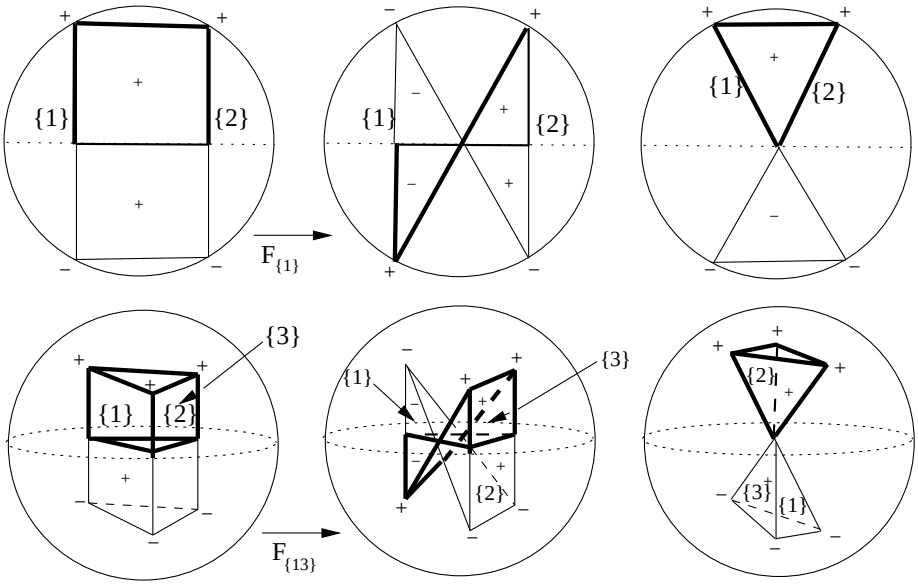

Figure 5: On the left, we have 2 and 3 dimensional convex prisms, followed by examples of convex prism-regions, which will be called *prisms*. We will denote such a prism as $|P, R|$. The convex prism in H^3 can be defined by placing a hyperbolic triangle in a hyperplane of H^3, and then taking the convex hull of the union of the geodesics perpendicular to the hyperplane that contains the vertices of this specified triangle. Via the labeling convention described in section 2.1, we can utilize the pictured hyperplanes in order to label the vertices as $\{ij\}^{\pm}$. As such, the labeled $\pm$ signs are sufficient to decorate our vertices. $||P, R||$ can be naturally cut in half, and each component of the interior of these halves has either positive or negative vertices in its closure. Hence, every prism has a well defined *top* associated to its positive vertices and a well and *bottom* associated to its negative vertices. In the figure, the top half is indicated with the bold face lines. In going from our left most to our middle prism we have demonstrated geometrically the notion of a flip, as introduced in section 2.1 .

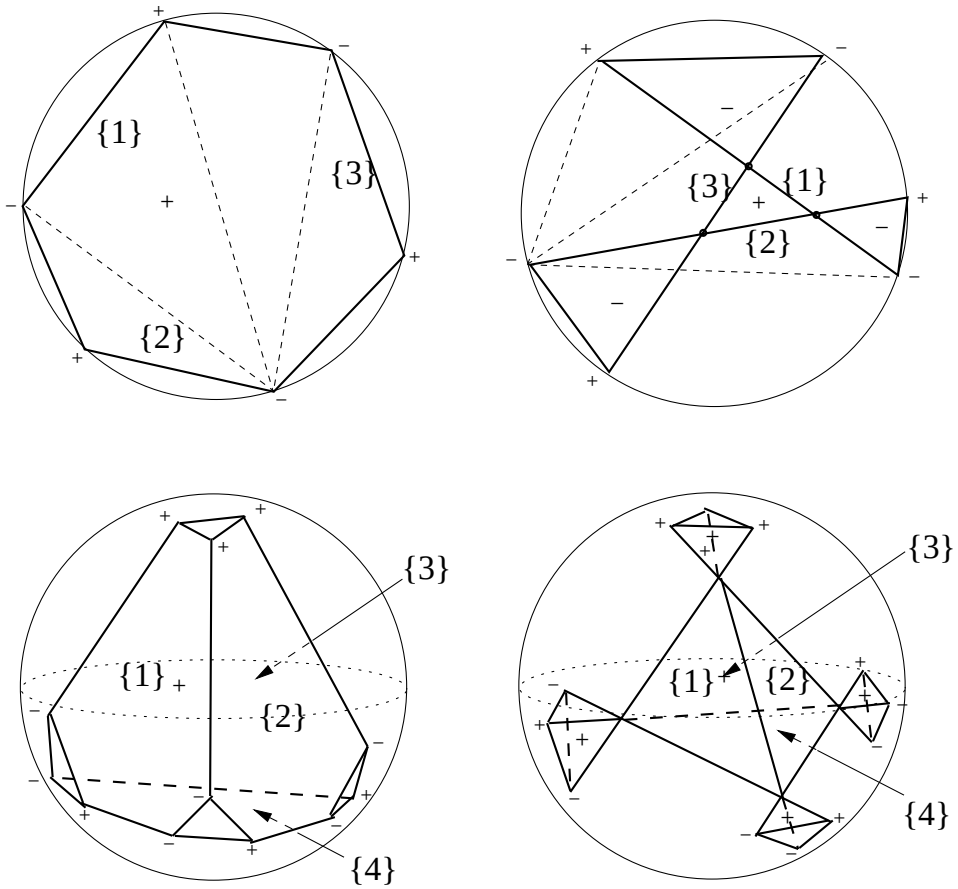

Figure 6: On the left, we have 2 and 3 dimensional convex supersimplicies, followed by examples of convex supersimplex-regions, which will be called *supersimplicies* and denoted $|Su, R|$. To construct a *supertetrahedron*, first take a Euclidean tetrahedron in the Klein model with all its vertices hyperideal, and with the property that each of its edges intersects H^3. The convex supertetrahedron can be defined as the convex hull of the geodesics formed by intersecting the Euclidean tetrahedron's edges with H^3, as indicated in the figure. Note, there are 4 natural prisms in a supertetrahedron. We have utilized the 4 labeled hyperplanes in order to label our supertetrahedron, and to each subset of 3 of these hyperplanes we have an associated a prism. We will let $|P, R_i|$ be the prism associated to the hyperplanes $\{1, 2, 3, 4\} - \{i\}$ with its top determined by the three vertices whose convex hull is a facet of the convex supertetrahedron.

accept

$$F_{ij}R(\{ij\}^{\pm}) = R(\{ij\}^{-\pm}).$$

We define ΩR be the new realization determined by flipping all of $|C, R|$'s edges.

Lemma 2 *The following facts are true about the 3 dimensional prism described in figure 5.*

1. *A prism is equivalent to a collection* 3 *decorated, non-degenerate planes.*
2. *A prism can be divided in to a top and bottom half, which are scissors congruent .*
3. *If we flip all the edges of a prism then the top half of the new prism is isometric to the top half of the original prism, and via an orientation reversing isometry.*

Proof: Given a prism $|P, R|$, since R satisfies the needed planarity constraints, we can construct the planes needed in the first part of this lemma. Conversely with these decorated planes we have determined where the vertices of C must go under R which, by lemma 1, completely determines our needed prism.

Given a prism the three planes it determines either intersect at a finite or hyperideal point (since R is injective the point cannot be ideal, see comment 2 at the end of this section). Hence, with a hyperbolic isometry we can send this point to infinity if it is hyperideal or to the origin in the Klein model this point is finite. Then, via edge flips, we can arrange this configuration of planes to be qualitatively either the first or final prism in row two of figure 5. In these two cases the prism's top and bottom are mirror images of each other, hence by equation (2), the top and bottom scissors congruent. Now we simply pick an ideal triangulation, and perform the edge flips to see that there is, up to orientation, only one other qualitatively distinct case, that of the middle prism in the second row of figure 5. This case also satisfies this mirror image property as needed. Notice that lemma 1 assures us that we need not examine what takes place with regard to other triangulation choices. One can also prove the second part by an induction from the 1 to the 2 to the 3 dimensional case and beyond. However, in even dimensions, the bottom half of the finite vertexed prism will have the opposite orientation of the top.

Having explicitly described all our prisms, the third part can simply be verified by picking an ideal triangulation, and explicitly performing the Ω transformation in the three qualitatively distinct cases. This third part is always true in odd dimensions. **q.e.d**

Lemma 3 *The following facts are true about the supertetrahedron described in figure 6.*

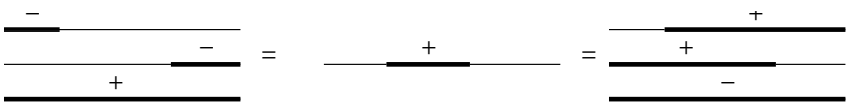

Figure 7: On the left we see a positively oriented one dimensional supersimplex and its 2 associated one dimensional prism halves, which are removed to form the simplex in the center of the figure. On the right, we see the consequence of performing an edge flip, which results in the same simplex, as needed.

1. *A supertetrahedron is equivalent to a collection* 4 *decorated, non-degenerate planes.*

2. *Every supertetrahedron determines* 4 *prisms, and the region determined by removing the top halves of these* 4 *prisms is independent of edge flips.*

Proof: The first part is proved exactly as the first part of lemma 2 was proved. That every supertetrahedron geometrically determines 4 prisms follows from the fact that our our supertetrahedron is equivalent to a collection 4 decorated planes, which provides us with the four collections of 3 decorated planes, needed to construct our prisms from lemma 2. That the region formed by removing the top halves of these 4 prisms is independent of edge flips can be proved much like the proof of lemma 1. Namely, we need only show that such a region has the same boundary before and after an edge flip. There are two types of boundary components. The part contained in the planes determined by the supertetrahedron and the hyperbolic triangles in the waists of the prisms when a triple of these planes intersect at a hyperideal point. The hyperbolic triangles in the second case are easily seen to be edge flip invariant by simply performing the needed flip to each of the 2 qualitatively different types of such prisms found in figure 5. To prove that the parts of the boundary contained in the planes determined by the supertetrahedron are preserved under edge flips is slightly trickier to verify directly. Namely, there are many cases to check, one such case is explicitly verified in figure 3. By lemma 1, we can use a single triangulation per case to check all the possibilities. However there are many cases. To circumvent this issue we can boot strap from the lower dimension examples. Namely, notice our needed result will follow if the corresponding fact is true for the 2 dimensional supertetrahedra in figure 6. Similarly, with this same reasoning, we find that the 2 dimensional fact is true provided the fact is true in one dimension. In one dimension the result is transparent, see figure 7. This inductive procedure can be easily suped up to imply the analogs of these results in all dimensions.

q.e.d

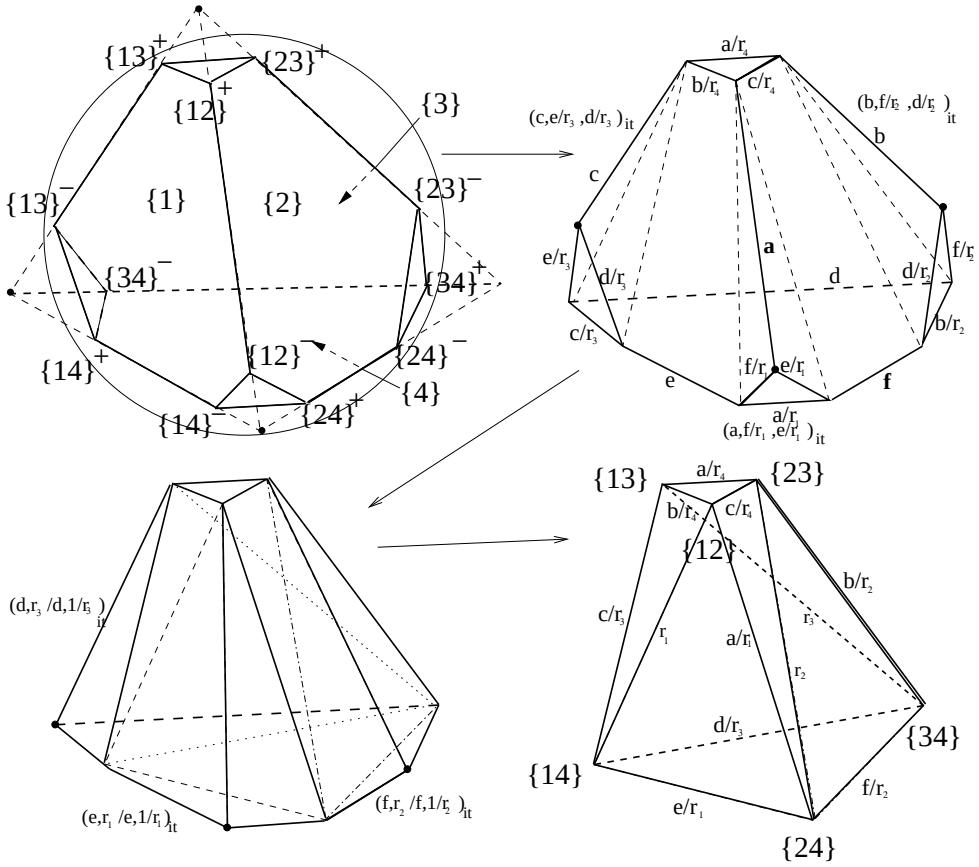

Figure 8: Here we cut down to one of the supertetrahedron's 2^6 hearts, namely the octahedron with the vertices $\{\{1,2\}^+, \{1,3\}^+ \{1,4\}^+, \{2,3\}^+, \{2,4\}^+, \{3,4\}^+\}$. This describes a C-region, $|H,R|$, determined from any supertetrahedron $|Su,R|$. We have also labeled the clinants of $|Su,R|$ and used these clinants to describe the clinants of $|H,R|$. We have also indicated all the ideal tetrahedra utilized to cut $|Su,R|$ down to $|H,R|$.

A Supertetrahedron's Heart: Given any convex ideal polyhedron, C, if a vertex is 3 valent, then we can cut off the ideal tetrahedron it determines, hence, determining a new convex ideal polyhedron in the process. A *cut down* of C , is a maximal sequence of such cuts. For example, cutting down the convex prisms in figure 5 results in the empty set. In figure 8, we see an example of cutting down a convex supertetrahedron to an ideal octahedron. Once we have a cut down of a convex ideal polyhedron C, we may utilize our cutting down procedure to cut down any C-region $|C, R|$. Cutting down a supertetrahedron always result in some nonempty polyhedron, which we will call one of C's *hearts*. If we take the set of edges, $E = \{\{ij\}\}$, then there are $2^{|E|}$ hearts of a convex supertetrahedron each given by the convex hull of the vertices $\{e^{sgn(e)}\}_{e\in E}$, where sgn is any of the $2^{|E|}$ mappings in the form

$$sgn : E \to \pm.$$

In fact, this construction makes sense with respect to a supersimplex in every dimensions, where there are still $2^{|E|}$ such hearts, and any heart of any supersimplex is combinatorially equivalent to the polyhedron in Euclidean space determined by taking the convex hull of the midpoints of the edges of the n-simplex, called the abosimplex by Conway. The ambotetrahedron happens to be the octahedron.

Theorem 4 *The following facts are true about the 3 dimensional generalized hyperbolic tetrahedron as described in figure 9.*

1. *A generalized hyperbolic Tetrahedron is equivalent to a non-degenerate collection* 4 *planes.*

2. $$2[T(Su, R)] = 2[Su, R] - \sum_i [P, R_i]. \tag{20}$$

$$2[T(Su, R)] = [Su, R] + [Su, \Omega(R)]. \tag{21}$$

$$2[T(Su, R)] = [H, R] + [H, \Omega(R)]. \tag{22}$$

Proof: Part 1 of this theorem follows from the second part of lemma 3 and the definition of the generalized hyperbolic Tetrahedron.

From lemma 2, the top and bottom halves of the prism are scissors congruent. This together with the definition of the generalized hyperbolic tetrahedron in figure 9, gives us formula 20. This fact is true in all dimensions.

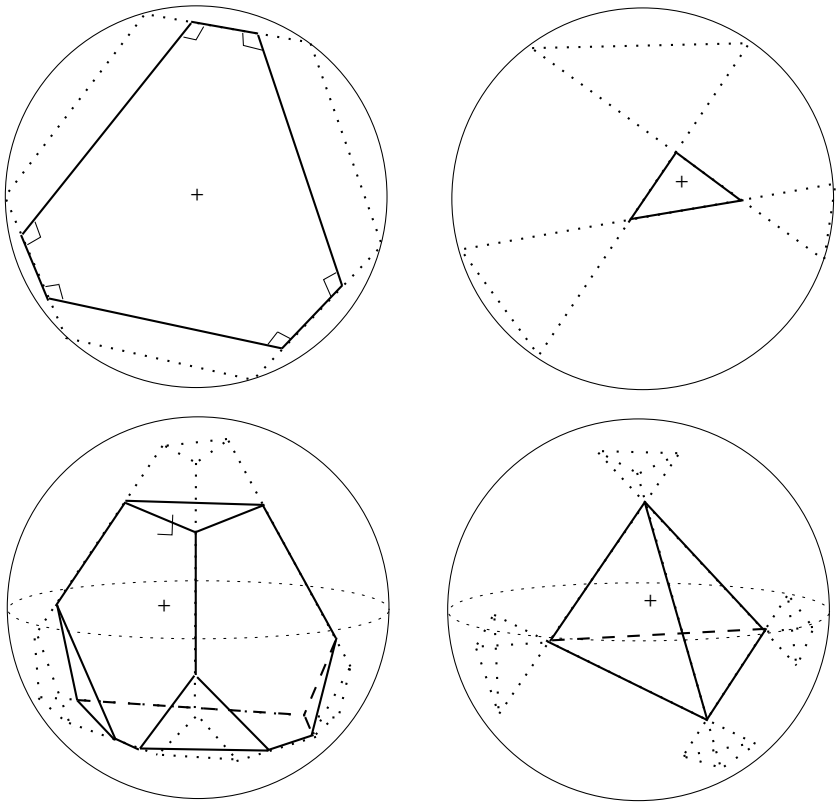

Figure 9: To define a generalized hyperbolic tetrahedron we use the fact from lemma 2 that each $|P, R_i|$ has a well defined top half and we utilize the second part of lemma 3, assuring us that we have a well defined region upon the removal from $|Su, R|$ of the four top half prisms defined by the $|P, R_i|$. A *generalized hyperbolic tetrahedron* is the geometric region determined by removing the top half of each $|P, R_i|$. As in this figure, the notion of a generalized hyperbolic tetrahedron coincides with the notion of a finite hyperbolic tetrahedron, when each triple intersection of the tetrahedral planes is non-empty. Let $T(Su, R)$ denote the generalized hyperbolic tetrahedron determined by $|Su, R|$, and let $[T(Su, R)]$ be $T(Su, R)$'s scissors class.

By lemma 2, $|P, R_i|$ is isometric, via an orientation reversing isometry, to $|P, \Omega(R)_i|$. Hence, the half prisms used to define our generalized hyperbolic tetrahedron cancel out as scissors classes, leaving us with equation (21). Using the cut down described in figure 8, we find the clinants of the ideal tetrahedron used to cut $|Su, R|$ down to $|H, R|$ are conjugate to those used to cut $|Su, \Omega(R)|$ down to $|H, \Omega(R)|$. Hence, by equation (12), the ideal tetrahedra utilized to cut down $[Su, R]$ and $[Su, \Omega(R)]$ occur in oppositely oriented pairs, and cancel out as scissors classes. Hence, equation (21) implies equation (22). Formulas (22) and (21) hold in all odd dimensions for the same reasons. **q.e.d**

Comment 1: Equation (20) in theorem 4 leads to interesting volume formula as well (see Mohanty [7] for a discussion of these volume formulas). Formula 1.1.3 will follow equation (22), together with the tools presented in section 2.3. Murakami and Yano present formula 1.1.3 together with a pair of other formula (see [8]) which follow from equation (20), together with the tools presented in section 2.3.

Comment 2: From theorem 4 we nearly have theorem 2 from section 1.2.1. However, in theorem 2 the condition that each $\{ijk\}$ is ideal has been dropped. To extend the notion of generalized tetrahedra to include ideal points, one could simply drop the R's injectivity condition, construct our supertetrahedra as just as in figure 6, and then remove only the hyperideal and finite half prisms as in figure 9. We will arrive at a well defined region which we can call a generalized hyperbolic tetrahedron. Such regions now include the possibility of ideal vertices and are in one to one correspondence with collections of four, distinct, labeled, pairwise intersecting planes in H^3, as need in theorem 2. There is a another version of this construction which is compatible with the constructions in sections 2.2 and 2.3. To discuss this construction, one must go outside the realm of C-regions altogether. First, observe that the union of a ideal tetrahedron and its positively oriented mirror image is a degenerate prism. Such a union occurs as the triangle in the waist of a convex prism, see figure 5, degenerates to a Euclidean triangle. We can visualize this degenerations by fixing the positions on the sphere at infinity of the vertices at the bottom of the prism. As we degenerate , we see a single ideal tetrahedron, the other becoming 'hidden' at infinity. Such prisms are in the appropriate compactification of the space of prisms. Similarly, at every ideal vertex of a supertetrahedron there is a 'hidden' ideal tetrahedra. Removing our 'hidden' half prisms will remove the supertetrahedron's hidden tetrahedra, hence, the resulting tetrahedron is still embedded and now has ideal points.

2.2 Octahedral Buddies

In this section, we will put coordinates on the space of supertetrahedra, introduced in section 2.1, and on the space of ideal octahedra, introduced in figure 10. Technically, when we discuss coordinates on a space we will mean that an open dense set of the coordinates we present form the coordinates of an open dense subset of our space. We shall also interpret mappings expressed in coordinates as restricted to the appropriate open dense subsets. We do this because our C-regions are only designed to capture an open dense set of the objects of interest to us here, and because we will need to move between descriptions of our spaces that utilize complex coordinates and descriptions utilizing various clinants. The need for such a convention can already be seen when describing the space of ideal tetrahedra, see the note at the end of section 1.1.2. In section 2.4, we will carefully describe the exact open dense subsets to which the geometric constructions presented in this paper apply without modification.

From figure 10, we see that an ideal octahedron can be decomposed into four ideal tetrahedra, hence utilizing the complex coordinates of these ideal tetrahedra, we find that set of all

$$\mathbf{w} = (w_1, w_4, w_3 w_4) \in \mathbf{C}^4$$

satisfying the *holonomy constraint* that

$$w_1 w_2 w_3 w_4 \quad = \quad 1 \tag{23}$$

form coordinates on the space of ideal octahedra. We shall now attempt to utilize the octahedron's clinants to find another set of coordinates. To do so, note, the dihedral clinants of an ideal octahedron are 12 unit complex number indexed by the edges of the convex octahedron that multiply to 1 at every vertex, and that multiply to 1 around each of the octahedron's 3 waists. The indexing of the octahedral clinants is discussed in figure 10, and we shall let $\mathbf{o}$ denote an element of $\times^{12} S^1$ that satisfies these octahedral constraints and is ordered as follows

$$\mathbf{o} = (\theta^{12}_{13}, \theta^{12}_{14}, \theta^{12}_{23}, \theta^{12}_{24}, \theta^{34}_{13}, \theta^{34}_{14}, \theta^{34}_{23}, \theta^{34}_{24}, \theta^{13}_{14}, \theta^{13}_{23}, \theta^{14}_{24}, \theta^{23}_{24}).$$

We shall see that such a $\mathbf{o}$ nearly determines an octahedron. To understand this claim it is useful to reparameterize our possible $\mathbf{o}$ via the coordinates introduced in figure 8. To accomplish this, first notice from figure 8, we see that for a suitable $(a, b, c, d, e, f; r_1, r_2, r_3, r_4)$ that that we can form an octahedron with clinants $\mathbf{o}(a, b, c, d, e, f; r_1, r_2, r_3, r_4)$ equal to

$$\left(\frac{b}{r_4}, r_1, \frac{c}{r_4}, \frac{a}{r_1}, r_3, \frac{d}{r_3}, \frac{b}{r_2}, \frac{f}{r_2}, \frac{c}{r_3}, \frac{a}{r_4}, \frac{e}{r_1}, r_2 \right).$$

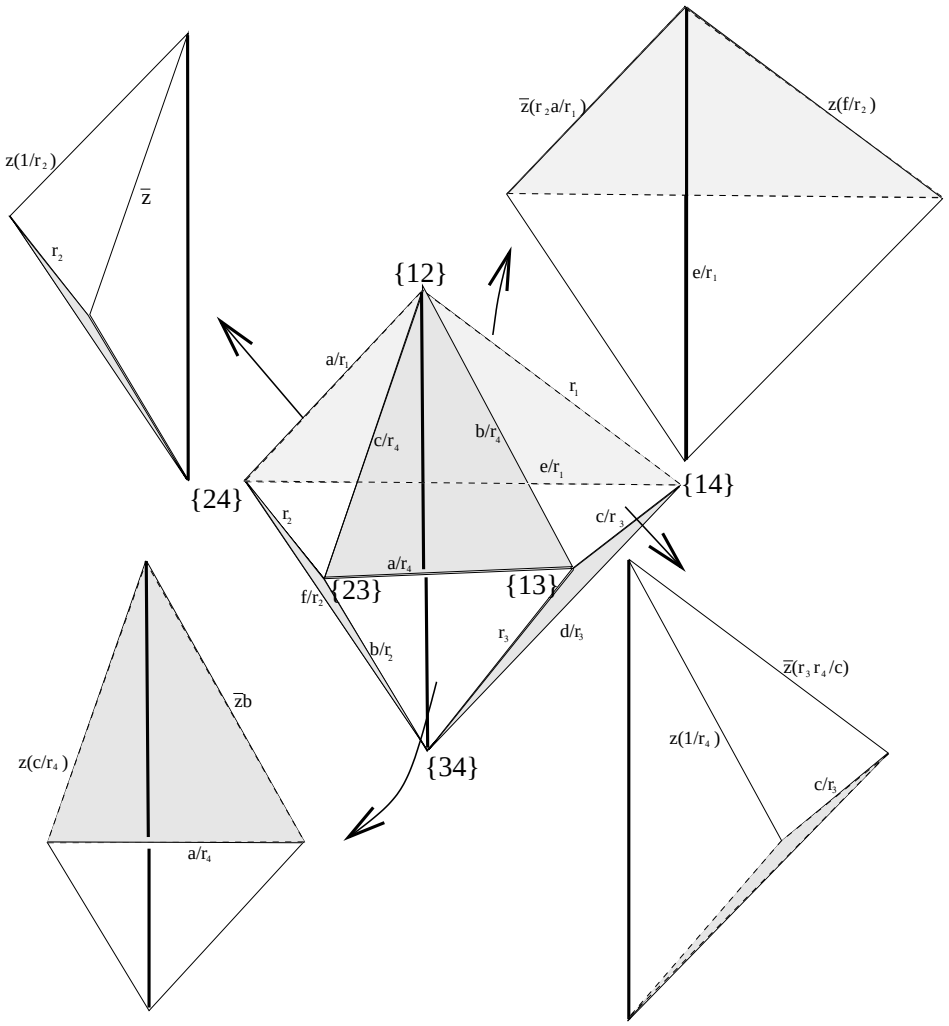

Figure 10: Here we see a convex ideal octahedron, O, in the Klein model, with a specified triangulation, S_o. Notice there are three such triangulations, each corresponding to choosing a pair of non-adjacent vertices. To each such triangulation there is also associated a *waist*, namely the four edges not containing either one of the specified pair of non-adjacent vertices. We let an ideal octahedron be any O-region, $|O, R|$. If we wish to discuss the clinants of an ideal octahedron we let θ^{ij}_{lk} denote the clinant associated to the edge with vertices $\{ij\}$ and $\{lk\}$. For example, in our figure $\theta^{12}_{13} = \frac{b}{r_4}$. As pictured, the ideal tetrahedral clinants of (S_o, R) are determined by the octahedron's dihedral clinants up to a single unknown clinant, labeled z.

Let us comment on these $(a,b,c,d,e,f;r_1,r_2,r_3,r_4)$ coordinates. To each $\{ij\}$ edge in figure 8 we have associated a clinant. The fact that the clinants at an ideal vertex multiply to one determine the r_i up to sign. Namely,

$$\begin{aligned} r_1^2 &= aef && (24)\\ r_2^2 &= bdf && (25)\\ r_3^2 &= cde && (26)\\ r_4^2 &= abc. && (27) \end{aligned}$$

There is also a condition on the r_i due to the fact that the clinants around an octahedron's waist multiply to one; namely

$$r_1 r_2 r_3 r_4 = abcdef. \quad (28)$$

We will let a coordinate in the form

$$\mathbf{s} = (a,b,c,d,e,f;r_1,r_2,r_3,r_4)$$

denote an element of $\times^{10} S^1$ that satisfies conditions 24-28. These can be used as a reparameterization of the octahedron's clinants since the mapping

$$\mathbf{s}(\mathbf{o}) = \left(\theta_{24}^{12}\theta_{14}^{12}, \theta_{34}^{23}\theta_{24}^{23}, \theta_{14}^{13}\theta_{34}^{13}, \theta_{34}^{14}\theta_{34}^{13}, \theta_{24}^{14}\theta_{14}^{12}, \theta_{34}^{24}\theta_{24}^{23}, \theta_{14}^{12}, \theta_{24}^{23}, \theta_{34}^{13}, \frac{1}{\theta_{13}^{12}\theta_{23}^{13}\theta_{23}^{12}}\right).$$

is easily checked to be $\mathbf{o}$'s inverse.

In figure 10, we see that the space of octahedra can be constructed from dihedral clinants once we have determined the clinant labeled z. If we let

$$(\mathbf{s},z)\hat{}_{\mathrm{MY}} = \left(\frac{1}{z}, \frac{z}{r_2}, \frac{b}{z}, \frac{zc}{r_4}, \frac{r_3 r_4}{zc}, \frac{z}{r_4}, \frac{ar_2}{zr_1}\frac{zf}{r_2}\right) \quad (29)$$

and let $(\mathbf{s},z)\hat{}_{\mathrm{MY}}(j)$ be the j^{th} component of $(\mathbf{s},z)\hat{}_{\mathrm{MY}}$, then, from equation (10), we have that the w_i coordinates of our ideal octahedron are equal to

$$w_i(\mathbf{s},z) = \frac{1-\overline{(\mathbf{s},z)\hat{}_{\mathrm{MY}}(2i)}}{1-(\mathbf{s},z)\hat{}_{\mathrm{MY}}(2i-1)}.$$

Notice if we let

$$(\mathbf{s})_{waist} = \left(r_2, \frac{a}{r_4}, \frac{c}{r_3}, \frac{e}{r_1}\right) \quad (30)$$

then by equation (13), for any unit sized z,

$$2[\mathbf{w}(\mathbf{s},z)] = [(\mathbf{s},z)\hat{}_{\mathrm{MY}}] + [(\mathbf{s})_{waist}] \quad (31)$$

To find the z that corresponds to our octahedron, notice that equation (23), implies that z must solve

$$k(\mathbf{s},z) \quad = \quad \Pi_{i=1}^{4}(1-\overline{\hat{(\mathbf{s},z)}_{\mathrm{MY}}(2i)}) - \Pi_{i=1}^{4}(1-\hat{(\mathbf{s},z)}_{\mathrm{MY}}(2i-1)) = 0. \quad (32)$$

Upon multiplying out this equation (23), we find that $(1/z)k(\mathbf{s},z)$ is a quadratic polynomial in z with coefficients in the supertetrahedral clinants. Hence an octahedron is determined by its $\mathbf{s}$ coordinate along with the correct root of $k(\mathbf{s},z)$. We will call the root, $\hat{\rho}$, corresponding to our octahedron the octahedron's *octahedral root*. In order, to understand the space of octahedron of fundamental importance is the following quantity:

$$\hat{\delta} = \frac{-4}{ab^2d} disc\left(\frac{k(\mathbf{s},z)}{z}\right),$$

where $disc$ refers to the quadratic's discriminant.

Lemma 4 *For any* $\mathbf{s}$ *we have that* $\hat{\delta}$ *is real and the open set of* $(\mathbf{s},\hat{\rho})$ *with* $\hat{\delta} > 0$ *form coordinates on the space of octahedra.*

Proof: Let $\mathbf{c} = (\mathrm{A},\mathrm{B},\mathrm{C},\mathrm{D},\mathrm{E},\mathrm{F}) \in \times^6 S^1$ and define

$$\mathbf{s}(\mathbf{c}) = (\mathrm{A}^2,\mathrm{B}^2,\mathrm{C}^2,\mathrm{D}^2,\mathrm{E}^2,\mathrm{F}^2,-\mathrm{AEF},-\mathrm{BDF},-\mathrm{CDE},-\mathrm{ABC}).$$

Via this mapping the $\mathbf{c}$ coordinates form a 2^3 fold cover of our $\mathbf{s}$ coordinates. Let Neg be the set of transformations that negate a collection of the $\mathbf{c}$ coordinates that share a face in figure 1. This cover's deck group is the copy of $\frac{\mathbf{Z}}{8\mathbf{Z}}$ generated by the elements of N. As a set, this deck group is $K_4 \bigcup Neg$, where K_4 is the group introduced in the comment at the end of section 1.2.1. We find that $k(\mathbf{s}(\mathbf{c}),z)$ can be expressed as

$$\hat{h}(\mathbf{c},z) = \frac{2}{\mathrm{AB}^2\mathrm{D}z} k(\mathbf{s}(\mathbf{c}),z) = \hat{\alpha}z^2 + 2\hat{\beta}z + \bar{\hat{\alpha}}$$

with

$$\bar{\hat{\alpha}}(\mathbf{c}) = 2\left(\frac{\mathrm{B}}{\mathrm{E}} + \mathrm{AD} + \mathrm{BE} + \mathrm{AB}^2\mathrm{D} + \mathrm{ABF} + \frac{\mathrm{AB}}{\mathrm{F}} + \mathrm{BCD} + \frac{\mathrm{BD}}{\mathrm{C}}\right)$$

and

$$\hat{\beta}(\mathbf{c}) = \frac{\mathrm{A}}{\mathrm{D}} + \frac{\mathrm{D}}{\mathrm{A}} + \frac{\mathrm{C}}{\mathrm{F}} + \frac{\mathrm{F}}{\mathrm{C}} + \mathrm{CF} + \frac{1}{\mathrm{FC}} - \left(\mathrm{AD} + \frac{1}{\mathrm{AD}} + \frac{\mathrm{B}}{\mathrm{E}} + \frac{\mathrm{E}}{\mathrm{B}} + \mathrm{BE} + \frac{1}{\mathrm{BE}}\right),$$

and notice β is real. These quantities are not independent of the choice of $\mathbf{c}$ satisfying $\mathbf{s}(\mathbf{c}) = \mathbf{s}$. Namely, $\hat{\alpha}(D\cdot\mathbf{c}) = -\hat{\alpha}(\mathbf{c})$, and that $\hat{\beta}(D\cdot\mathbf{c}) = -\hat{\beta}(\mathbf{c})$ when

$D \in N$, while the other deck transformations preserve these quantities. In particular,

$$\hat{\delta}(\mathbf{c}) = |\hat{\alpha}|^2 - \hat{\beta}^2,$$

is real and dependent only on $\mathbf{s}$. Furthermore when $\hat{\delta} > 0$ we have that

$$\hat{\rho}(\mathbf{c}) = \frac{-\hat{\beta} - i\sqrt{\hat{\delta}}}{\hat{\alpha}}.$$

and $\hat{\rho}(D \cdot \mathbf{c})$ are the two root of $\hat{h}(\mathbf{c}, z)$. Both these roots are unit sized since

$$|\hat{\rho}|^2 = \frac{\hat{\beta}^2 + \hat{\delta}}{\hat{\alpha}\bar{\hat{\alpha}}} = \frac{|\hat{\alpha}|^2}{|\hat{\alpha}|^2} = 1.$$

Hence when $\hat{\delta} > 0$ we can generically construct our needed ideal tetrahedra. Now when $\hat{\delta} < 0$ we have that $\hat{h}(\mathbf{c}, z)$'s roots are given by

$$\frac{-\hat{\beta} \pm \sqrt{\hat{\delta}}}{\hat{\alpha}},$$

and, hence, have magnitude

$$\frac{\hat{\beta}^2 + \hat{\delta} - 2\beta\sqrt{\hat{\delta}}}{\hat{\alpha}\bar{\hat{\alpha}}} = 1 \pm \frac{2\beta\sqrt{\hat{\delta}}}{|\hat{\alpha}|^2},$$

which is not not unit sized, since $\delta < 0$ implies that $\beta^2 > 0$, hence for $\beta\sqrt{\hat{\delta}}$ to be equal to 0, we need that $\delta = 0$.

q.e.d

We will freely replace the coordinate $(\mathbf{s}, \hat{\rho})$ of an ideal tetrahedron with a $(\mathbf{c})$, as introduced in the proof of lemma 4, where $\mathbf{s}(\mathbf{c}) = \mathbf{s}$ and $\hat{\rho}(\mathbf{c}) = \hat{\rho}$. We will say that $(\mathbf{c})$ is a choice of *tetrahedral circulants* associated to $(\mathbf{s}, \hat{\rho})$. Notice the tetrahedral circulants form a 4 fold cover of the $(\mathbf{s}, \hat{\rho})$ with nontrivial deck transformations given by the transformations that negate all the tetrahedral clinants except those corresponding to an opposite pair of edges. These are the geometrically trivial transformations which arose in the sketch of theorem 3's proof. Let $(\mathbf{c})_{oct}$ denote the octahedron with tetrahedral circulants $(\mathbf{c})$. Let

$$(\mathbf{c})_{op} = ((\mathbf{c})_{oct}, (\bar{\mathbf{c}})_{oct})$$

be called an pair of *octahedral buddies* .

Lemma 5 *The $(\mathbf{s}, \hat{\rho})$ with $\hat{\delta} > 0$ form coordinates on the space of all octahedral buddies ,*

$$2[(\mathbf{c})_{op}] \quad = \quad [\widehat{(\mathbf{c})_{MY}}] + \left[\widehat{(\bar{\mathbf{c}})_{MY}}\right], \tag{33}$$

$$\left[(\bar{\mathbf{c}})_{op}\right] \quad = \quad [(\mathbf{c})_{op}], \tag{34}$$

and if $D \in Neg$, then D commutes with conjugation,

$$[(D \cdot \bar{\mathbf{c}})_{oct}] \quad = \quad -[(\mathbf{c})_{oct}], \tag{35}$$

and

$$[(D \cdot \mathbf{c})_{op}] \quad = \quad -[(\mathbf{c})_{op}]. \tag{36}$$

Proof: That the $(\mathbf{s}, \hat{\rho})$ with $\hat{\delta} > 0$ form coordinates on the space of octahedral buddies follows immediately from lemma 4. Equation (33) follows from equation (31) and equation (12). Equation (34) follows from the definition of $(\mathbf{c})_{op}$. We mention it in order to emphasize that conjugation does **not** correspond to reversing orientation. Instead $D \in Neg$ does the job of reversing orientation job, even on the level of the octahedron. To see this notice that if we conjugate every clinant in figure 10 then we arrive at $(D \cdot \bar{\mathbf{c}})_{oct}$, since $\hat{\rho}(D \cdot \bar{\mathbf{c}}) = \overline{\hat{\rho}\,(\bar{\mathbf{c}})}$. Hence, equation (35) follows form this observation together with equation (12). The equation (36) follows from equations (34) and (35).

q.e.d

Generically, we can geometrically invert an octahedron back into a supertetrahedron utilizing the ideal tetrahedra in figure 8. In particular, by lemma 4, the coordinates $(\mathbf{c})$ with $\hat{\delta} > 0$ will cover the space of generalized hyperbolic tetrahedron. We will denote the tetrahedron corresponding to such a coordinate as $(\mathbf{c})_{tet}$.

Lemma 6 *Generically,*

$$2[(\mathbf{c})_{tet}] \quad = \quad [(\mathbf{c})_{op}]. \tag{37}$$

Proof: Let $|Su, R|$ be the supertetrahedron generically corresponding to $(\mathbf{c})$, and so

$$(\mathbf{c})_{oct} = |H, R|.$$

Since $|H, \Omega(R)|$'s is an octahedron with dihedral clinants $\overline{\mathbf{d}}(\mathbf{c})$, either $|H, \Omega(R)| = (\bar{\mathbf{c}})_{oct}$ or $|H, \Omega(R)| = (D \cdot \bar{\mathbf{c}})_{oct}$ with $D \in Neg$. If $|H, \Omega(R)| = (D \cdot \bar{\mathbf{c}})_{oct}$ Then

$|H, \Omega(R)|$ has all its tetrahedral clinants conjugate to those of $|H, R|$, and hence by equation (12),

$$[H, R] + [H, \Omega(R)] = 0.$$

This, generically, contradicts equation (22), hence $|H, \Omega(R)| = (\bar{\mathbf{c}})_{oct}$ and

$$(|H, R|, |H, \Omega(R)|) = (\mathbf{c})_{op}.$$

q.e.d

Comment: Notice that when $\delta = 0$, that we have a unique unit root $\hat{\beta}/\hat{\alpha}$ of $\hat{h}(\mathbf{c}, z)$. Hence are still in a position to construct our octahedra. In this case, we find that all our 4 tetrahedral planes intersect in a point, which corresponds to an infinitesimal hyperbolic tetrahedron, or rather a Euclidean tetrahedron. One nice way to understand this is to note that $\delta = -16 \det(Gr)$, where Gr is the Graham matrix associated to our planes. Hence $\delta = 0$ exactly when we are in the Euclidean case.

2.3 The Group

We introduce the group described in theorem 3. It will be generated by the puff-and-cuts in in figure 11. These puff-and-cuts take an octahedron $|O, R|$ and transform it into $|O, P_v^F R|$. For every vertex face pair this induces a mapping of the octahedral clinants, which we shall dente as $P_v^F \mathbf{o}$. For example, letting F be the face of our octahedron with $F = \{\{12\}, \{13\}, \{23\}\}$ we have $P_{\{12\}}^F \mathbf{o}$ equals

$$P_{\{12\}}^F \mathbf{o} = \left(\frac{1}{\theta_{14}^{12}}, \frac{1}{\theta_{13}^{12}}, \frac{1}{\theta_{24}^{12}}, \frac{1}{\theta_{23}^{12}}, \theta_{13}^{34}, \theta_{14}^{34}, \theta_{23}^{34}, \theta_{24}^{34}, \theta_{14}^{13}\theta_{13}^{12}\theta_{14}^{12}, \theta_{23}^{13}, \theta_{24}^{14}, \frac{\theta_{24}^{23}}{\theta_{13}^{12}\theta_{14}^{12}} \right).$$

We can express this transformation in the supertetrahedral coordinates as

$$P_{\{12\}}^F \cdot \mathbf{s} = \mathbf{s}(P_{\{1,2\}}^F(\mathbf{o}(\mathbf{s}))) = \left(\frac{1}{a}, b, c, d, e, f, \frac{r_1}{a}, r_2, r_3, \frac{r_4}{a} \right).$$

Let $22.5\mathrm{K}$ denote the group generated by the P_v^F, as in the sketch of theorem 3's proof. Geometrically, we will be most interested in the action of $22.5\mathrm{K}$ when viewed as acting on octahedral buddies . We explore $22.5\mathrm{K}$'s algebraic structure in section 2.3.2, for now we need the following lemma.

Lemma 7 *For $g \in G$ we generically have*

$$[(\mathbf{c})_{op}] = [(g \cdot \mathbf{c})_{op}], \tag{38}$$

$$(\overline{g \cdot \mathbf{c}}) = (g \cdot \bar{\mathbf{c}}). \tag{39}$$

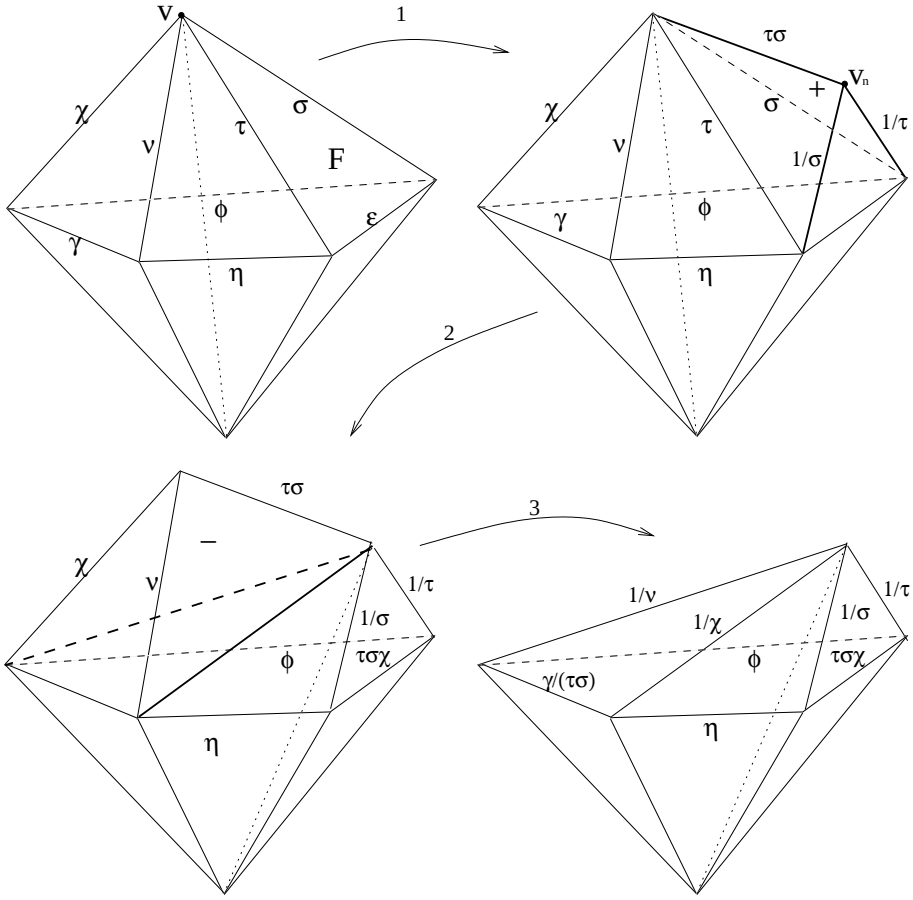

Figure 11: We start by describing the puff of $|O, R|$ with respect to a vertex, v, and face, F, with $v \in F$. If we assume $\tau\sigma \neq 1$, then F's neighboring faces at v intersect in a geodesic, pictured as the edge with the $\tau\sigma$ clinant attached to it after step 1. Using this geodesic we may determine a new ideal vertex, the vertex labeled v_n. A *puff* is the operation of adjoining the ideal tetrahedron $(1/\tau, 1/\sigma, \tau\sigma)_t$ that contains v_n and F, as pictured after step 1. After our puff, v becomes a trivalent vertex, as in step 2. Being a trivalent vertex, we may *cut* v off, as seen in step 3. Equivalently, we may change R to $P_v^F R$ by demanding that $P_v^F R(p) = v_n$ for the for the p such that $R(p) = v$, and letting $R(q) = P_v^F R(q)$ for every other octahedral vertex q. We say $|O, P_v^F R|$ results from $|O, R|$ via a *puff-and-cut*.

Proof: Notice that the clinants of

$$(\mathbf{c})_{oct} = |H, R|$$

and

$$(\bar{\mathbf{c}})_{oct} = |H, \Omega(R)|$$

are conjugates, hence the ideal tetrahedra utilized in figure 11 to transform $(\mathbf{c})_{op}$ to

$$(|H, P_v^F R|, |H, P_v^F \Omega(R)|) = (P_v^F \cdot \mathbf{c})_{op}$$

will cancel out as scissors classes, by equation (12).

To prove equation (39), note we either have equation 39 or

$$(g \cdot \bar{\mathbf{c}}) = (D \cdot \overline{g \cdot \mathbf{c}})$$

for $D \in Neg$. Notice by equation 36 that

$$[(D \cdot \overline{g \cdot \mathbf{c}})_{op}] = -[(\overline{g \cdot \mathbf{c}})_{op}].$$

By the definition of $g \in G$ and equation 34 we have

$$\begin{aligned} [(g \cdot \bar{\mathbf{c}})_{op}] &= [g \cdot (\bar{\mathbf{c}})_{op}] \\ &= [g \cdot (\mathbf{c})_{op}] \\ &= [(g \cdot \mathbf{c})_{op}] \\ &= [(\overline{g \cdot \mathbf{c}})_{op}] \end{aligned}$$

Hence, $(\overline{g \cdot \mathbf{c}}) \neq (D \cdot \overline{g \cdot \mathbf{c}})$ and equation (39) follows.

q.e.d

The 24 possible puff-and-cuts in figure 11 are the generators of $22.5\mathrm{K}$. It is straight-forward to verify that the opposite faces at a vertex induces the same transformation of the $\mathbf{s}$ coordinate. From this, these transformations induce the same transformation of the octahedral buddies , due the following scholium to lemma 7.

Lemma 8 *How $g \in G$ acts on $(\mathbf{c})_{op}$ is completely determined by how g acts on $\vec{d}(\vec{t})$.*

Proof: The $\mathbf{c}$ coordinate representing $g \cdot \mathbf{s}$. is either $g \cdot \mathbf{c}$ or $D \cdot g \cdot \mathbf{c}$ with $D \in Neg$. But

$$[(g \cdot \mathbf{c})_{op}] = -[(D \cdot g \cdot \mathbf{c})_{op}]$$

hence, by lemma 7, generically only one of $g \cdot \mathbf{c}$ or $D \cdot g \cdot \mathbf{c}$, can represent a image of $(\mathbf{c})_{op}$ under $22.5\mathrm{K}$.

q.e.d

Hence, $22.5\mathrm{K}$ is generated by twelve of the P_v^F. These generators break naturally into two class, those with a *shaded face* in figure 10, and those with an *unshaded* face in figure 10. Hence we will simply denote P_v^F as P_v^u or P_v^s depending on whether we are using one of the shaded or unshaded faces at v. For example, our above $P^F_{\{1,2\}} = P^s_{\{1,2\}}$, since we utilized a shaded face. As with our $P^s_{\{1,2\}}$ transformation, in the tetrahedral coordinates all of our shades transformation simply invert the clinant corresponding to v. In terms of our supertetrahedral coordinates, we have

$$P^F_{\{12\}} \cdot \mathbf{s} = \left(\frac{1}{a}, b, c, d, e, f, \frac{r_1}{a}, r_2, r_3, \frac{r_4}{a}\right) \tag{40}$$

$$P^s_{\{34\}} \cdot \mathbf{s} = \left(a, b, c, \frac{1}{d}, e, f, r_1, \frac{r_2}{d}, \frac{r_3}{d}, r_4\right) \tag{41}$$

$$P^s_{\{23\}} \cdot \mathbf{s} = \left(a, \frac{1}{b}, c, d, e, f, r_1, \frac{r_2}{b}, r_3, \frac{r_4}{b}\right) \tag{42}$$

$$P^s_{\{14\}} \cdot \mathbf{s} = \left(a, b, c, d, \frac{1}{e}, f, \frac{r_1}{e} r_2, \frac{r_3}{e}, r_4\right) \tag{43}$$

$$P^s_{\{13\}} \cdot \mathbf{s} = \left(a, b, \frac{1}{c}, d, e, f, r_1, r_2, \frac{r_3}{c}, \frac{r_4}{c}\right) \tag{44}$$

$$P^s_{\{2,4\}} \cdot \mathbf{s} = \left(a, b, c, d, e, \frac{1}{f}, \frac{r_1}{f}, \frac{r_2}{f}, r_3, r_4\right). \tag{45}$$

These shaded elements generate the group isomorphic to $\left(\frac{\mathbf{Z}}{2\mathbf{Z}}\right)^6$ discussed in proof of corollary 2, which we will call the *shaded subgroup*. If our octahedron is $|H, R|$ for some supertetrahedron $|Su, R|$, then P_v^s applied to our octahedron corresponds to $|H, F_v R|$. In other words, P_v^s corresponds to flipping the v edge of $|Su, R|$. In particular, by theorem 4, the shaded subgroup preserves not only the scissor class of the tetrahedron but the underlying tetrahedron itself. In fact, recall from section 2.2 that the space of octahedral buddies covers the generalized hyperbolic tetrahedra. The shaded subgroup is the group of deck transformations of this cover.

The unshaded transformations are much more geometrically subtle. Algebraically they are given by the following transformations.

$$P^u_{\{12\}} \cdot \mathbf{s} = \left(a, \frac{r_4}{r_1}, \frac{r_1 r_4}{a}, d, \frac{e r_4}{b r_1}, \frac{f r_4}{b r_1}, \frac{r_4}{b}, \frac{r_3}{e}, r_3, r_4\right) \tag{46}$$

$$P^u_{\{34\}} \cdot \mathbf{s} = \left(a, \frac{r_2}{r_3}, \frac{c r_2}{b r_3}, d, \frac{e r_2}{b r_3}, \frac{r_2 r_3}{d}, r_1, r_2, \frac{r_2}{b}, \frac{r_1}{e}\right) \tag{47}$$

$$P^u_{\{23\}} \cdot \mathbf{s} = \left(\frac{r_2 r_3}{b}, b, \frac{r_4}{r_2}, \frac{d r_4}{c r_2}, e, \frac{f r_4}{c r_2}, r_1, \frac{r_4}{c}, \frac{r_1}{f}, r_4\right) \tag{48}$$

$$P^u_{\{14\}} \cdot \mathbf{s} = \left(\frac{a r_3}{c r_1}, b, \frac{r_3}{r_1}.\frac{r_1 r_3}{e}, e, \frac{f r_3}{c r_1}.\frac{r_3}{c}.r_2, r_3, \frac{r_2}{f}\right) \tag{49}$$

$$P^u_{\{13\}} \cdot \mathbf{s} = \left(\frac{r_4}{r_3}, \frac{r_3 r_4}{c}, c, \frac{d r_4}{a r_3}, \frac{e r_4}{a r_3}, f, \frac{r_2}{d}, r_2, \frac{r_4}{a}, r_4\right) \tag{50}$$

$$P^u_{\{24\}} \cdot \mathbf{s} = \left(\frac{r_1}{r_2}, \frac{b r_1}{a r_2} c, \frac{d r_1}{a r_2}, \frac{r_1 r_2}{f}, f, r_1, \frac{r_1}{a}, r_3, \frac{r_3}{d}\right) \tag{51}$$

2.3.1 Proof of Theorem 1

We can now use $22.5\mathrm{K}$ to prove theorem 1. Namely, we use the fact that g_o from the sketch of the proof of theorem 1 is in $22.5\mathrm{K}$. In fact, if we let s_1 and s_2 be the elements of the shaded subgroup determined by

$$s_1 \cdot \mathbf{s} = \left(\frac{1}{a}, \frac{1}{b}, c, \frac{1}{d}, \frac{1}{e}, f, \frac{r_1}{ae}, \frac{r_2}{bd}, \frac{r_3}{de}, \frac{r_4}{ab}\right)$$

$$s_2 \cdot \mathbf{s} = \left(a, b, \frac{1}{c}, d, \frac{1}{e}, f, \frac{r_1}{e}, r_2, \frac{r_3}{ce}, \frac{r_4}{c}\right).$$

then

$$g_o = s_2 P^u_{\{3,4\}} s_1.$$

Note

$$g_o \cdot \mathbf{s} = \left(\frac{1}{a}, \frac{d}{r_2 r_3}, \frac{e r_2}{b r_3}, \frac{1}{d}, \frac{b r_3}{c r_2}, \frac{r_2}{r_3}, \frac{b}{r_4}, \frac{1}{r_3}, \frac{e}{r_3}, \frac{1}{r_4}\right).$$

We chose g_o so that we could take the hat off $\hat{\rho}$ from section 2.2. In other words, we have the following lemma.

Lemma 9

$$\rho(\mathbf{c}) \quad = \quad \hat{\rho}(g_o \cdot \mathbf{c})$$

Proof: This nearly follows by direct substitution. The nearly refers to the fact that by direction substitution we find for each $\mathbf{c}$ that $\rho(\mathbf{c}) = \hat{\rho}(g_o \cdot \mathbf{c})$ or $\rho(\mathbf{c}) = \hat{\rho}(g_o \cdot (D \cdot \mathbf{c}))$, with $D \in Neg$. By continuity of the construction with respect to the parameters, we need to verify the formula for an element of each of the connected components of the subset of $\mathbf{c}$ coordinates where $\hat{\delta} > 0$. There are only two such components which are related by the transformation sending $\mathbf{c}$ to $D \cdot \mathbf{c}$, and the formula is easily verified.

q.e.d

From lemma 9 and a direct substitution we have that

$$(g_o \cdot \mathbf{c})\hat{}_{\mathrm{MY}} \quad = \quad (\mathbf{c})_{\mathrm{MY}}. \tag{52}$$

We may now prove theorem 1, by noting that generically

$$\begin{array}{rcll} 4[(\mathbf{c})_{tet}] & = & 2[(\mathbf{c})_{op}] & \text{by equation 37} \\ & = & 2[(g_o \cdot \mathbf{c})_{op}] & \text{by equation 38} \\ & = & [(g_o \cdot \mathbf{c})\hat{}_{\mathrm{MY}}] + \left[(\overline{g_o \cdot \mathbf{c}})\hat{}_{\mathrm{MY}}\right] & \text{by equation 33} \\ & = & [(g_o \cdot \mathbf{c})\hat{}_{\mathrm{MY}}] + \left[(g_o \cdot \bar{\mathbf{c}})\hat{}_{\mathrm{MY}}\right] & \text{by equation 39} \\ & = & [(\mathbf{c})_{\mathrm{MY}}] + [(\bar{\mathbf{c}})_{\mathrm{MY}}] & \text{by equation 52.} \end{array}$$

2.3.2 An Algebraic Description of $22.5\mathrm{K}$

To expose the algebraic structure of $22.5\mathrm{K}$ it is useful to introduce some new coordinates. Recall that to resolve the branching necessary to determine $\hat{\rho}$ from $\mathbf{s}$ we only need a two fold cover of $\mathbf{s}$, not the 2^3 fold cover determined by the $\mathbf{c}$ coordinates. We now describe this cover. Let $\mathbf{b} = (t, u, v, T, U, V; r) \in \times^7 S^1$ such that $r^2 = (tuv)/(TUV)$. We can send a $\mathbf{c}$ coordinate to such a coordinates via

$$\mathbf{b}(\mathbf{c}) = \left(\mathrm{AD}, \mathrm{BE}, \mathrm{CF}, \mathrm{D}/\mathrm{A}, \mathrm{E}/\mathrm{B}, \mathrm{F}/\mathrm{C}, -\mathrm{ABC}\right),$$

and we can send a $\mathbf{b}$ coordinate to a $\mathbf{s}$ coordinate via

$$\mathbf{s}(\mathbf{b}) = (t/T, u/U, v/V, tT, uU, vV, UVr, TUrTVr, r).$$

As such, we find that the the tetrahedral circulants cover the balanced coordinates via 4 fold cover (as described in the comment at the end of section 1.2.1) and the balance coordinates cover the $\mathbf{s}$ coordinates via a 2 fold cover, given by negating t, u, v, T, U and V and leaving r alone. We will call this transformation D, and

note that $\mathbf{b}(\hat{D} \cdot \mathbf{c}) = D \cdot \mathbf{b}(\mathbf{c})$, when $\hat{D} \in Neg$. From this identity, the balanced coordinates parametrize our octahedral buddies .

Using the balanced coordinates, we provide an explicit algebraic description of the group $22.5\mathrm{K}$ from section 1.2.2. To do so, we first lift the action on the $\mathbf{s}$ coordinate described by equations (40)-(51) to a transformation of the balanced coordinates. We will index our group elements by how they act on $(t, u, v, T, U, V; r)$. Using the same argument as found in lemma 9, we can then determine whether our lift or D times our lift represents the needed transformation. We find the shaded elements are given by

$$\{[\bar{T}, u, v, \bar{t}, U, V; r], [T, u, v, t, U, V; T\bar{t}r], [t, U, v, T, u, V; U\bar{u}r]$$

$$, [t, u, V, T, U, v; V\bar{v}r], [t, \bar{U}, v, T, \bar{u}, V; r], [t, u, \bar{V}, T, U, \bar{v}; r]\} .$$

while the unshaded elements are given by

$$\{[U, u, v, T, t, V; U\bar{t}r], [\bar{U}, u, v, T, \bar{t}, V; r], [t, V, v, T, U, u; V\bar{u}r],$$

$$[t, \bar{V}, v, T, U, \bar{u}; \bar{u}\bar{V}r], [t, u, T, v, U, V; T\bar{v}r], [t, u, \bar{T}, \bar{v}, U, V; \bar{v}\bar{T}r]\} .$$

Note the action on r is determined by the action on the first 6 coordinates, and that r does not affect the action upon the first six coordinates. Hence to identify the group we only need to understand $22.5\mathrm{K}$'s action on the (T, u, v, t, U, V) coordinates. Each of these generators is a permutations of the $\mathbf{b}$ coordinates together with something in the group generated by conjugating an even number of the $\mathbf{b}$ coordinates. In fact, these elements are easily checked to generate this group. This is a well known reflection group usually denoted as D_6.

Note: In the $\mathbf{b}$ coordinates

$$\alpha(\mathbf{b}) = 2(t + u + v + tuv - r(T + U + V + TUV)),$$

$$\beta(\mathbf{b}) = (T + U + V + 1/T + 1/U + 1/V) - (t + u + v + 1/t + 1/u + 1/v).$$

$$\vec{\gamma}(\mathbf{b}) = [r, 1, rTU, tu, rTV, tv, rUV, uv].$$

Due to the simple nature of $22.5\mathrm{K}$ in the balanced coordinates, it is easy to explore $22.5\mathrm{K}$'s action on these quantities. For example, by plugging in the above generators, we find that δ is $22.5\mathrm{K}$ invariant.

2.3.3 Scissors Cosets

With the balanced coordinates we can easily describe our 30 scissors classes described in the proof of corollary 2. From equation 2, the scissor classes described in corollary 2 occur in pairs consisting of a tetrahedron and its mirror image. Hence,

we only need to describe fifteen scissors classes no pair of which are mirror images of each other. In other words, we need to describe the cosets of the quotient of $22.5\mathrm{K}$ by the group generated by the tetrahedral symmetries together with the shaded subgroup. To do so, we let a lower and capital case coordinate pair in (t, u, v, T, U, V), like t and T, be called a *pair*. The shade subgroup in balanced coordinates is generated by the transformations that swap the elements of a pair, for example $TuvtUV$, and the elements that conjugate a pair, for example $\bar{t}uv\bar{T}UV$. The group of tetrahedral symmetries is generated by permuting the pairs, for example $utvUTV$, together with the transformations that conjugate a pair of the capitol letters, for example $tuv\bar{T}\bar{U}V$. Together, the shaded subgroup and tetrahedral symmetries form a group generated by all pair swaps, all pair permutations, together with all even conjugations. Hence the needed cosets are indexed by the elements of the following sets:

$$SR = \{tuvTUV, tuvTVU, tuvUTV, tuvUVT, tuvVTU, tuvVUT\},$$

together with

$$SN = \{tuTvVU, tuTvUV, tuUvTV, tvTuVU, tvTuUV,\ tvUuTV,$$

$$uvTtVU, uvTtUV, uvUtTV, \}\,,$$

where the group elements have been indexed by how they act on (t, u, v, T, U, V). We distinguished between these two subsets since the SR corresponds to the 6 nontrivial Regge scissors classes, which, in the $\mathbf{b}$ coordinates, is the group generated by independently permuting the lower or upper case coordinates together with the even conjugations of the uppercase coordinates. SN corresponds to the remaining 9 nontrivial scissors classes.

2.4 The Generic Set

We will now describe an open dense set of the octahedral buddies where all the construction needed to prove theorems 1 and 3 are guaranteed to apply. Namely, we will restrict the $g \cdot \mathbf{b}$ to where the 8 ideal tetrahedra from figure 10 and the 6 ideal tetrahedra arising when inverting $(g \cdot \mathbf{b})_{oct}$ to a supertetrahedron, as in figure 8, are non-degenerate for all $g \in G$. When all such tetrahedra are nondegenerate, all our construction make sense with out modification.

Lemma 10 *Suppose all images of r under $22.5\mathrm{K}$ are nondegenerate, then the ideal tetrahedra forming $(g \cdot \mathbf{b})_{oct}$, as in figure 10, are nondegenerate for every $g \in G$.*

Proof: We need to check that all the tetrahedral clinants of $(\mathbf{b})_{oct}$ are nondegenerate under this assumption. Note that the $22.5\mathrm{K}$ images of r under $22.5\mathrm{K}$ are the 'positive' square roots of all the even conjugations applied to $tuvTUV$. The waist has clinants which are all in this form. To see that the remaining tetrahedral clinants are nondegenerate, note that the z from figure 10 satisfies equation 32, and, hence,

$$\Pi_{i=1}^{4}(1-\overline{(\mathbf{s}(\mathbf{b}),z)\hat{}_{\mathrm{MY}}(2i)}) \;=\; \Pi_{i=1}^{4}(1-(\mathbf{s}(\mathbf{b}),z)\hat{}_{\mathrm{MY}}(2i-1)). \qquad (53)$$

Notice the $(\mathbf{s}(\mathbf{b}),z)\hat{}_{\mathrm{MY}}(j)$ are our need tetrahedral clinants, up to conjugation. Let us assume one of these clinants is degenerate and produce a contradiction. Under this assumption to one side of equation (53) is equal to zero. If one side is zero then the other has to be zero, hence, have a degenerate term as well. So, for some i and j

$$(\overline{(\mathbf{s}(\mathbf{b}),z)\hat{}_{\mathrm{MY}}(2i)})(\mathbf{s}(\mathbf{b}),z)\hat{}_{\mathrm{MY}}(2j-1)=1. \qquad (54)$$

Upon multiply this expression out, we find that the right hand side of equation (54) is an image of r under $22.5\mathrm{K}$, our needed contradiction.

q.e.d

This lemma assures us that when acting on the octahedral buddies that we never run into a degeneracy in the compliment of the set determined by the 16 monomial constraints derived from $r=1$ under $22.5\mathrm{K}$'s action. Notice these clinants correspond to supertetrahedral dihedral clinants under the edge flips alone. Hence, none are found in the interior of the collection of the octahedral buddies corresponding to the finite tetrahedra and all there images under $22.5\mathrm{K}$. This is a useful observation, for it tells us that if we look at the image of the space finite tetrahedra under $g\in G$, then whether a triple of planes intersects at a finite or hyperideal point is the same for the image of every finite tetrahedron. Clearly the group generated by the shaded subgroup and the tetrahedral symmetries satisfy that such intersections occur at finite vertices. Hence, we can understand every element of $22.5\mathrm{K}$ by examining the 15 cosets in section 2.3.3. We find that the 6 Regge cosets in SR preserve the fact that all the planes intersect at finite points, while the remaining 9 cosets have all 4 triples of planes intersecting at hyperideal points.

Lemma 11 *Suppose no clinant derived from r or tT via the action of $22.5\mathrm{K}$ is degenerate, then the ideal tetrahedra utilized when forming the supertetrahedron from $(g\cdot\mathbf{b})_{oct}$, as in figure 8, are nondegenerate for every $g\in G$.*

Proof: The clinants of these tetrahedron are either an image of r under $22.5\mathrm{K}$ or supertetrahedral clinant along a tetrahedral edge. By the definition of the balance

coordinates the supertetrahedral clinants along a tetrahedral edge are in the form of an element of $22.5\mathrm{K}$ applied to tT, as needed.

q.e.d

From lemmas 10 and 11, we will never run into a degenerate tetrahedron when working in the set where (t, u, v, T, U, V) is in the compliment of the set determined by the 46 monomial constraints derived from $tT = 1$ and $r = 1$ under $22.5\mathrm{K}$'s action.

Comment: In relatively straight-forward ways, the constructions presented in section 2.1 and 2.2 can be extended to much of the set where an image of r or tT under the action of $22.5\mathrm{K}$ is degenerate. However, attempts at finding a unified approach have not been successful. In order to make good geometric sense out of these constructions in general, we must take the correct compactification of the set of $\mathbf{b}$ where our constraints are nondegenerate. This will force us to go beyond the C-regions, see the note at the end of section 2.1. The above constraints eliminate many interesting cases, like a tetrahedron with ideal vertices and any tetrahedron exhibiting a symmetry where, for example, $\mathrm{AB} = \mathrm{DE}$.

3 Derivation of Equation (18)

Recall from section 1.1.4, that to derive equation (18), we first derive equation (19), which we do in section 3.1. Then we check that $\mathcal{H}(w)$ is odd, which is verified in section 3.2.

3.1 Derivation of Equation (19)

The first step in proving equation (19) is the geometric rearrangement of octahedral buddies as described in figure 12. In this section, we will assume α, β, and γ are evaluated at ${g_o}^{-1} \cdot \mathbf{b}$ which is equivalent to the hats in section 2.2. From figure 12, we have that

$$2[(\mathbf{b})_{op}] \quad = \quad \sum_{i=1}^{8} (-1)^i [z_i(\mathbf{b})]. \tag{55}$$

and, utilizing equation (10), we have

$$z_j(\mathbf{b}) = \frac{1 - \gamma_j \eta}{1 - \gamma_j \eta^c}.$$

The $\mathbf{z}$ form coordinates on the space of octahedral buddies that reside in the following set:

$$\mathcal{DT} = \left\{ \mathbf{z} \in \mathbf{C}^8 \left| \Pi_i^4 \frac{z_{2i-1}}{z_{2i}} = 1, \Pi_i^4 \frac{1 - z_{2i-1}}{1 - z_{2i}} = 1, Im\left(\frac{z_i}{z_j}\right) = 0 \right. \right\}.$$

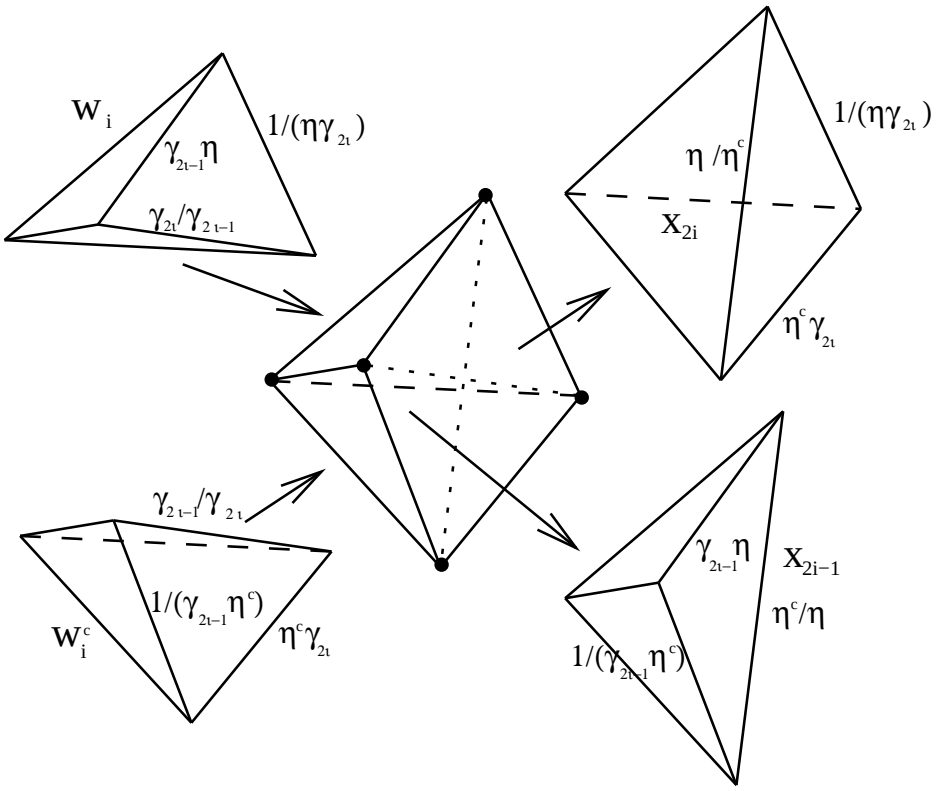

Figure 12: On the left hand side of this figure we have a pair of the ideal tetrahedra arising in the description of $(\mathbf{b})_{op}$. To be precise, we have pictured $w_i(\mathbf{b})$, labeled as w_i, and $w_i(\bar{\mathbf{b}})$, labeled as w_i^c. We have labeled the tetrahedral clients using the $\vec{\gamma}$ from section 1.1.4, evaluated at ${g_o}^{-1} \cdot \mathbf{b}$, or rather $\vec{\gamma}({g_o}^{-1} \cdot \mathbf{b}) = \left(1, \frac{1}{r_2}, \frac{1}{b}, \frac{c}{r_4}, \frac{c}{r_3 r_4}, \frac{1}{r_4}, \frac{r_1}{a r_2} \frac{f}{r_2}\right)$. We glue our w_i and w_i^c together in order to form the C-region in the middle of this picture. We then resplit this C-region to construct the labeled x_j complex coordinates. We let $z_{2i-1} = 1/x_{2i-1}$ and $z_{2i} = x_{2i}$. Let us denote the list of 8 ideal tetrahedra indexed by these z_i as $\mathbf{z} \in \mathbf{C}^8$. We chose to let z_{2i-1} to be one over the x_{2i} coordinate of the tetrahedron in the lower right corner of our figure so that all the z_j share the same clinant, η/η^c, where $\eta = \hat{\rho}(\mathbf{b})$ and $\eta^c = \overline{\hat{\rho}(\bar{\mathbf{b}})}$.

Conversely, by inverting the construction in figure 12, the elements of $\mathcal{DT}$ can be used to form octahedral buddies . Hence, the $\mathbf{z}$ in $\mathcal{DT}$ parameterize the octahedral buddies .

Given a complex number z we let $z/|z|$ be called its associated *circulant* and $z/\bar{z}$ be called its associated *clinant*. The condition $\Im\left(\frac{z_i}{z_j}\right) = 0$ is equivalent to the fact that all our z_i have the same clinant associated to them, η/η^c as seen in figure 12. We will call this the *magic clinant*. The magic clinant is preserved by an order-2304 subgroup $H < G$ described in section 3.3. Representatives of the ten right cosets of H in $22.5\mathrm{K}$ index ten truly distinct volume formulas. These cosets are explicitly described in section 3.3.

Since every angle of an octahedron is on the waist with respect to some simplicial decomposition, the octahedron, unlike our other C-regions, has well defined circulants. From figure 12, we know that the z_i share the same clinant. However, the z_i will not, in general, share the same circulant. For convex supertetrahedron, by explicitly performing the construction in figure 8, we find that the even and odd z_i have circulants that differ by a minus sign. In fact, both the octahedral buddies corresponding to a convex supertetrahedron are convex, have the same orientation and one has dihedral angles that are π minus the other's dihedral angles. As another example, when we cut down a standard finite vertexed supertetrahedron we find that the resulting z_i have circulants that all agree. In fact, by explicitly performing the construction in figure 8, one of the octahedral buddies corresponding to a standard finite vertexed supertetrahedron is the opposite orientation of the other and has negated dihedral angles. Hence, the finite tetrahedra correspond to a subset of

$$\mathcal{FT} = \left\{ \mathbf{z} \in \mathbf{C}^8 \left| \Pi_i^4 \frac{z_{2i-1}}{z_{2i}} = 1, \Pi_i^4 \frac{1 - z_{2i-1}}{1 - z_{2i}} = 1, \frac{z_1}{z_j} > 0 \right. \right\}.$$

We now derive formula (19). Notice that from equation (7), that

$$\mathcal{B}(z) = -\mathcal{B}(1-z) = -\Im(\mathcal{L}_2(1-z) + I \arg(z) \log|1-z|).$$

Hence, from equations (55) and (9), we have that

$$\mathcal{V}(2[(\mathbf{b})_{tet}]) = -\sum_{i=1}^{8} (-1)^i \mathcal{B}(1 - z_i).$$

If we restrict our selves to $\mathcal{FT}$, then all the z_i circulants are the same, and the fact that

$$\Pi_i^4 \left| \frac{1 - z_{2i-1}}{1 - z_{2i}} \right| = 1$$

assures us that we can ignore the $\arg(z)\log|1-z|$ part of $\mathcal{B}$. Hence we have

$$\mathcal{V}(2[(\mathbf{b})_{tet}]) = -\Im\left(\sum_{i=1}^{8}(-1)^i\mathcal{L}_2(1-z_i)\right).$$

For $\mathbf{z}$ in $\mathcal{DT}-\mathcal{FT}$ the circulants don't agree and we will have to tack on $\pm I\pi\log(z)$ terms. For simplicity we will derive our formulas in the $\mathcal{FT}$ case. In this case, the fact that

$$\Pi_i^4\left|\frac{z_{2i-1}}{z_{2i}}\right| = 1.$$

assures us that

$$\Im\left(\sum_{i=1}^{8}(-1)^i\log(z_i)^2\right) = 0.$$

(we use the $\log(z)$ with $\log(1)=0$ and a branch cut along $(-\infty,0]$). Hence,

$$\mathcal{L}(z) = \mathcal{L}_2(1-z) + \frac{1}{4}\log(z)^2,$$

is an analytic function (with a branch cut along $(-\infty,0]$ and $\mathcal{L}(1)=0$) such that

$$\mathcal{V}(2[(\mathbf{b})_{tet}]) = \Im(\sum_{i=1}^{8}(-1)^i\mathcal{L}(z_i)).$$

Now we let

$$\mathcal{H}(w) = \mathcal{L}\left(\frac{1-w}{1+w}\right),$$

with branch cuts $[-\infty,1]\bigcup[1,\infty]$ and $H(0)=0$. Note $\frac{1-w}{1+w}$ is its own inverse and

$$\begin{aligned}\frac{1-z_i}{1+z_i} &= \frac{\gamma_i(\eta-\eta^c)}{2-\gamma_i(\eta+\eta^c)}\\ &= \frac{-\gamma_i(2i\sqrt{\delta}/\alpha)}{2+2\gamma_i(\beta/\alpha)}\\ &= \frac{-i\gamma_i\sqrt{\delta}}{\alpha+\gamma_i(\beta)}\\ &= \sqrt{\delta}c_i\end{aligned}$$

Where

$$c_i({g_o}^{-1}\cdot\mathbf{b}) = \frac{-i\gamma_i}{\alpha+\gamma_i\beta}.$$

Hence

$$\begin{aligned}\mathcal{L}(z_i) &= \mathcal{H}\left(\frac{1-z_i}{1+z_i}\right)\\ &= \mathcal{H}\left(c_i\sqrt{\delta}\right)\end{aligned}$$

We nearly have equation (18). Namely, everything has been evaluated at ${g_o}^{-1}\cdot \mathbf{b}$, hence we must apply g_o. A priori, there is a possibility that we will need to tack on tack on $\pm I\pi\log(z)$ terms to our $\mathcal{L}$. To assures ourselves that we do not need to, we must check that the $z_i/z_j > 0$ constraint is preserved under the g_o transformation. Such a constraint can only changes signs if an ideal tetrahedra in $(\mathbf{b})_{op}$ degenerates. By lemma 10, this cannot occur in the connected set of finite tetrahedra, hence cannot occur in any image of this set under $22.5\mathrm{K}$. So we only need to verify this for a single finite tetrahedron, which is easily accomplished.

Comment 1: In this section, we see that we only need the generalized tetrahedra in $\mathcal{FT} \subset \mathcal{DT}$ in order to derive equation (16). The finite tetrahedra are a proper subset of $\mathcal{FT}$ and generalized tetrahedra are still necessary. For example, the transformation g_o will send any finite hyperbolic tetrahedron to a tetrahedron with tetrahedral planes that intersect at hyperideal points.

Comment 2: The $\mathcal{DT}$ parameterization of our octahedral buddies makes transparent many of our $22.5\mathrm{K}$ symmetries. Namely, $\mathcal{DT}$ is clearly preserved by independently permuting the even and odd indexed z_i, by the transformation that sends the z forming $\mathbf{z}$ to $\frac{1}{\bar{z}}$, and by the transformation that conjugates and swaps the z_{2i-1} and z_{2i} terms. These transformations clearly preserve scissors class and, in fact, generate the H subgroup of $22.5\mathrm{K}$ discussed in section 3.3.

3.2 $\mathcal{H}(w)$ is odd

Notice that $H(w)$ is odd if $\mathcal{L}(z)$ from section 3.1 satisfies

$$\mathcal{L}\left(\frac{1}{z}\right) = -\mathcal{L}(z). \tag{56}$$

In order to prove equation (56), first we define

$$\mathcal{K}(z) = \frac{\mathcal{L}_2(1-z) - \mathcal{L}_2(1-1/z)}{2} \tag{57}$$

which clearly satisfies

$$\mathcal{K}\left(\frac{1}{z}\right) = -\mathcal{K}(z). \tag{58}$$

Hence, equation (56) will follow from the following lemma.

Lemma 12

$$\mathcal{L}(z) = \mathcal{K}(z)$$

Proof: This lemma will follows if we can demonstrate that

$$\mathcal{L}_2(1-1/z) \quad = \quad -\mathcal{L}_2(1-z) - \frac{1}{2}\log(z)^2. \tag{59}$$

To prove equation (59), we rewrite equation (59) as

$$\mathcal{L}_2(1-1/z) + \mathcal{L}_2(1-z) \quad = \quad -\frac{1}{2}\log(z)^2 \tag{60}$$

and note that the right and left hand sides of equation (60) are equal to 0 at $z = 1$. Hence we need only show that

$$d\left(\mathcal{L}_2(1-z) + \mathcal{L}_2(1-1/z)\right) = \frac{-1}{2} d\log(z)^2$$

We compute the left hand side

$$\begin{aligned} d(\mathcal{L}_2(1-z) + \mathcal{L}_2(1-\frac{1}{z})) &= -\log(z)d(\log(1-z)) - \log(1/z)\, d(\log(1-1/z)) \\ &= -\log(z)d(\log(1-z)) + \log(z)d\left(\log\left((z-1)/z\right)\right) \\ &= -\log(z)d(\log(z)) \end{aligned}$$

and find it is $\frac{-1}{2} d\log(z)^2$ as needed.

q.e.d

Comment: Equation (56) is very suggestive with regards to the Chern Simons invariant, but this turns out to be misleading since the scissors congruence taking $\mathbf{z}$ to $\frac{\mathbf{1}}{\bar{\mathbf{z}}}$, requires using the fact that $[z] = -[\bar{z}]$, which destroys the type of orientation-sensitivity needed to capture the Chern Simons invariant (see Neumann [10]).

3.3 10 Interesting Formulas

Once one has a volume formula in hand one can re-write this formula in many ways utilizing $22.5\mathrm{K}$, as described in section 2.3.2. For example we have that

$$\mathcal{V}([(\mathbf{b})_{tet}]) = \sum_{i=1}^{8} (-1)^i \mathcal{L}(z_i(g \cdot (\mathbf{b})_{tet}))$$

for every $g \in G$. What really distinguishes these different formulas is the magic clinant, as introduced in section 3.1. The magic clinant can be easily explored in the $\mathbf{b}$ coordinates by noting

$$\eta(\mathbf{b})/\eta(\mathbf{b})^c = \left(\frac{-\beta + i\sqrt{\delta}}{\alpha}\right)\left(\frac{-\beta + i\sqrt{\delta}}{\bar{\alpha}}\right) = \frac{(\beta^2 - \delta) - i(2\beta\sqrt{\delta})}{|\alpha|^2}$$

or rather

$$m(\mathbf{b}) \quad = \quad \frac{(\beta^2 - \delta) - i(2\beta\sqrt{\delta})}{|\alpha|^2}. \tag{61}$$

In particular, we can explore the subgroup of $22.5\mathrm{K}$ that preserves the magic clinant. Let H_0 be the subgroup generated by independently permuting the lower and upper case coordinates and performing an even number of conjugations. Since, as in the note at the end of section 2.3.2, all $g \in G$ preserve δ, and H_0 clearly preserve β, we have that H_0 must must preserve $|\alpha|^2$. Hence, from equation (61), H_0 preserves the magic clinant. Similarly, the transformation that swaps all pairs simultaneously (as defined in section 2.3.3) will negate β. Hence, this transformation conjugates the magic clinant. Let H is be the order-2304 subgroup generated by this swap transformation and H_0. The elements of $22.5\mathrm{K}$ not in H will not preserve the magic clinant. From this observation, we arrive at 10 truly distinct volume formulas index by G/H, with coset representatives given by

$$\{tuvTUV, TuvtUV, tUvTuV, tuVTUv, tvVTuU$$

$$, tTVuUv, tTuUvV, tTUuvV, tuUTvV, tTvuUV\}.$$

4 Questions

Question 1: Numerically, equation (16) holds in the spherical case and, by the analytic continuation principle, this is not very surprising. However, one finds that some of the constructions presented here become difficult to implement in the spherical case. Can these constructions be made to make sense in the spherical world? In particular, can one prove theorem 1 in the spherical case?

Question 2: Notice the scissor group produced here has been explicitly described when it is acting between pairs of tetrahedra. In order reduce to the tetrahedra, we are forced to use equation 1. Dupont and Sah's division algorithm, utilized to prove equation 1, is rather complicated to implement geometrically (see [2]). Is there a simple way to accomplish this division in this case?

Acknowledgments: The authors like to thank Yana Mohanty, Dylan Thurston, and Walter Neumann for the useful discussions we had with them concerning this work.

References

[1] Y. Cho and H. Kim. On the volume formula for hyperbolic tetrahedron. *Discrete and Computational Geometry*, 22:347–366, 1999.

[2] J. L. Dupont and C. H. Sah. Scissor congruences, 2. *Journal of Pure and Applied Algebra*, 25:159–195, 1982.

[3] J. L. Dupont and C. H. Sah. Three questions about simplices in spherical and hyperbolic 3-space. *The Gelfand Mathematical Seminars,1996-1999*, pages 49–76, 2000.

[4] R. Kellerhals. On the volume of hyperbolic polyhedra. *Mathematische Annalen*, 285:541–569, 1989.

[5] J. Milnor. Hyperbolic geometry: the first 150 years. *Bulletin of the American mathematical Society*, 6:9–24, 1982.

[6] J. Milnor. On polylogarithms, Hurwitz zeta functions, and the Kubert identities. *L'Enseignement Mathematique*, 29:281–322, 1983.

[7] Y. Z. Mohanty. The Regge symmetry is a scissors congruence in hyperbolic space. *Algebraic and Geometric Topology*, 3:1–31, 2003.

[8] J. Murakami and M. Yano. On the volume of a hyperbolic and spherical tetrahedron. *pre-print*, 2002.

[9] J. Roberts. Classical 6j-symbols and the tetrahedron. *Geometry and Topology*, 3:21–66, 1999.

[10] Neumann W. D. Hilbert's 3rd problem and invariants of 3-manifolds. *Geometry and Toplogy*, 1:383–410, 1998.